Journal of Medicinal Chemistry

Article

Structure-Activity Relationships of a Diverse Class of Halogenated Phenazines that Targets Persistent, Antibiotic-Tolerant Bacterial Biofilms and Mycobacterium tuberculosis

Aaron T. Garrison, Yasmeen Abouelhassan, Verrill M Norwood, Dimitris Kallifidas, Fang Bai, Minh Thu Nguyen, Melanie Rolfe, Gena M. Burch, Shouguang Jin, Hendrik Luesch, and Robert William Huigens III

J. Med. Chem., **Just Accepted Manuscript** • DOI: 10.1021/acs.jmedchem.5b02004 • Publication Date (Web): 28 Mar 2016

ACS Publications

Journal of Medicinal Chemistry is published by the American Chemical Society. 1155 Sixteenth Street N.W., Washington, DC 20036

Structure-Activity Relationships of a Diverse Class of Halogenated Phenazines that Targets Persistent, Antibiotic-Tolerant Bacterial Biofilms and *Mycobacterium tuberculosis*

Aaron T. Garrison[†⊥], Yasmeen Abouelhassan[†⊥], Verrill M. Norwood IV[†⊥], Dimitris Kallifidas[†⊥], Fang Bai[‡], Minh Thu Nguyen[†⊥], Melanie Rolfe[†⊥], Gena M. Burch[†⊥], Shouguang Jin[‡], Hendrik Luesch[†⊥], Robert W. Huigens III*[†⊥]

[†]*Department of Medicinal Chemistry, College of Pharmacy, University of Florida, Gainesville, Florida 32610;* [‡]*Department of Molecular Genetics & Microbiology, College of Medicine, University of Florida;* [⊥]*Center for Natural Products, Drug Discovery and Development (CNPD3), University of Florida*

Abstract. Persistent bacteria, including persister cells within surface-attached biofilms and slow-growing pathogens lead to chronic infections that are tolerant to antibiotics. Here, we describe the structure-activity relationships of a series of halogenated phenazines (HP) inspired by 2-bromo-1-hydroxyphenazine **1**. Using multiple synthetic pathways, we probed diverse substitutions of the HP scaffold in the 2-, 4-, 7- and 8-positions providing critical information regarding their antibacterial and bacterial eradication profiles. Halogenated phenazine **14** proved to be the most potent biofilm-eradicating agent (≥99.9% persister cell killing) against MRSA (MBEC < 10 μM), MRSE (MBEC = 2.35 μM) and VRE (MBEC = 0.20 μM) biofilms while **11** and **12** demonstrated excellent antibacterial activity against *M. tuberculosis* (MIC = 3.13 μM). Unlike antimicrobial peptide mimics that eradicate biofilms through the general lysing of membranes, HPs do not lyse red blood cells. HPs are promising agents that effectively target persistent bacteria while demonstrating negligible toxicity against mammalian cells.

INTRODUCTION

Current antibiotics operate primarily through growth-dependent mechanisms and suffer from an inability to effectively treat persistent and chronic infections involving bacterial biofilms (surface-attached communities) [1-4] and *Mycobacterium tuberculosis* (MtB).[5] Bacteria prefer to exist in biofilms that are composed of specialized, non-replicating persister cells encased within an extracellular matrix of biomolecules and demonstrate tolerance toward every class of antibiotic therapy.[4,6,7] Antibiotic tolerance is an innate bacterial phenotype attributed to metabolically dormant persister cells and distinct from acquired antibiotic resistance gained by rapidly-dividing, free-floating (planktonic) bacteria induced by antibiotic treatment (Figure 1).[6,8,9] Chronic and recurring bacterial infections are attributed to antibiotic tolerance which results in an estimated 17 million new biofilm infections and >500,000 annual deaths in the United States.[10,11] An unproductive antibiotic pipeline over the last 45 years has led to many BigPharma companies eliminating or significantly downsizing antibacterial discovery programs.[12] In addition, we have only begun to understand the importance of biofilms in human health over the last 20 years and currently there are no biofilm- or persister-eradicating therapeutics available to effectively treat chronic infections. In order to address persistent and biofilm-associated bacterial infections, innovative strategies are required to identify novel small molecules capable of targeting and killing non-replicating persister cells through unique, growth-independent mechanisms.

Many efforts have been made to modulate bacterial biofilms through the perturbation of bacterial signaling (quorum sensing) processes[13] or the identification of non-growth altering biofilm inhibitors and dispersal agents[11]; however, very few classes of biofilm-eradicating agents have been reported.[14-18] Unlike biofilm inhibitors and dispersal agents, biofilm-eradicating agents kill persister cells within surface-attached biofilms and have the potential to be stand-alone therapeutics for the treatment of biofilm-associated infections. The most prevalent class of biofilm-eradicating agents are the antimicrobial peptides (AMPs) and mimics thereof, which operate through bacterial membrane disruption and lysis.[14-18] The development of AMP-based antibacterial therapeutics is indeed promising; however, effective AMPs must target bacterial membranes over mammalian cell membranes to reduce or eliminate potential human toxicity concerns. New biofilm-eradicating agents that operate through complimentary mechanisms are critical to address biofilm-associated bacterial

infections and have the potential to address other problems associated with chronic bacterial infections, such as targeting slow-growing *Mycobacterium* infections.

The marine environment is an extensive source of microbial diversity and new antibacterial agents,[19] thus it is fertile ground for the discovery of antibacterial agents that operate through new modes of action and could lead to effective biofilm-eradicating agents. Marine sources have provided diverse classes of natural products able to modulate quorum sensing,[20-23] inhibit biofilm formation and/or disperse established biofilms.[11,24] Recently, our group found that 2-bromo-1-hydroxyphenazine **1**[25] (Figure 2), a phenazine originally isolated by Cushman and co-workers from a marine *Streptomyces* species, demonstrates potent antibacterial activity against *Staphylococcus aureus* and *S. epidermidis* (minimum inhibitory concentration or MIC of 6.25 μM; 1.7 μg/mL).[26] The antibacterial potency of this marine phenazine antibiotic is enhanced with a second bromine atom installed at the 4-position of the phenazine heterocycle (**2**[25,26]; MIC 0.78-1.56 μM, or 0.27-0.55 μg/mL against *S. aureus* and *S. epidermidis*).[26] Halogenated phenazine (HP) **2** displayed effective eradication activity against methicillin-resistant *Staphylococcus aureus* (MRSA) biofilms (minimum biofilm eradication concentration or MBEC ~ 150 μM).[27] In addition, we recently reported the identification of a small series of HP analogues that demonstrated potent biofilm eradication activities (MBEC = 0.2-12.5 μM) against several major human pathogens, including: MRSA, MRSE and VRE.[28] Here, we report the full account of our investigations detailing the chemical synthesis, biological evaluation and structure-activity relationships of a series of 29 HP analogues.

RESULTS AND DISCUSSION

Chemical Synthesis of Marine Halogenated Phenazine Analogues.

Our chemical synthesis efforts were motivated by our preliminary success in identifying potent biofilm-eradicating agents, and thus, newly synthesized HP analogues would be evaluated in an array of biological assays. Our initial goals were to synthesize a focused, yet diverse set of marine phenazine analogues with a primary emphasis on functionalizing the 7- and 8-positions (Figure 2) of the phenazine heterocycle. These synthetic goals can be achieved through the following transformations: (1) condensation between a quinone and

phenylenediamine[25,28] and (2) Wohl-Aue[29] condensation between anilines and nitroarenes. In addition, we were interested in probing alternative substitution patterns with various combinations of halogens and alkyl substituents of the phenazine scaffold which required multiple synthetic pathways (Scheme 1).

We began our chemistry efforts by synthesizing dichlorinated and diiodinated versions of HP **2** (Scheme 1.A). Although the dibromination reaction of 1-hydroxyphenazine was high-yielding when using *N*-bromosuccinimide (NBS; 99% yield),[26] the synthesis of 2,4-dichloro-1-hydroxyphenazine **3** and 2,4-diiodo-1-hydroxyphenazine **4** from 1-hydroxyphenazine **42** gave considerably lower yields. Chlorination at the 2- and 4-positions of 1-hydroxyphenazine using *N*-chlorosuccinimide (NCS) proceeded in a 47% yield to give **2** while iodination using *N*-iodosuccinimide (NIS) yielded **3** in only 19%. We also synthesized a series of mixed halogenated analogues **5-10** via a regioselective monohalogenation reaction at the 4-position of 1-methoxyphenazine **32** to give phenazines **33-35** (68-76% yield), followed by demethylation using boron tribromide (BBr_3) to give phenazine intermediates **39-41** (86-97% yield). A final halogenation reaction at the 2-position of 1-hydroxyphenazines **39-41** yielded mixed halogenated analogues **5-10** (34-91% yield).

1-Methoxyphenazines **20**, **30**, and **31** (synthesized via quinone-phenylenediamine condensation; see Supporting Information) were demethylated using boron tribromide to afford 1-hydroxyphenazines **21**, **43**, and **44** in 78-99% yield (Scheme 1.A). A dibromination reaction at the 2- and 4-positions of the phenazine heterocycle was carried out using two equivalents of *N*-bromosuccinimide (NBS) to afford HP analogues **16, 17** and **19** in 38-84% yield.[28] This synthetic approach enabled us to access key HP analogues with diversity at the 7- and 8-positions of the phenazine ring; however, the dibromination reaction with NBS proved to be troublesome and gave inconsistent results (i.e., low yields, impurities difficult to remove) during these studies.

To circumvent the problems encountered during the dihalogenation reaction, we used 1-methoxyphenazines **20**, **30** and **31** to sequentially install a single halogen atom at the 4-position of the phenazine ring upon treatment with one equivalent of halogenating agent (NCS, NBS, NIS or $KI/NaIO_4$) to give phenazines **36-38** in 59-96% yield (Scheme 1.A). Following this monohalogenation reaction at the 4-position, 1-methoxyphenazines **36-38** were demethylated using boron tribromide to yield 1-hydroxyphenazines **11-13** in 91-97% yield. Final

halogenation at the 2-position of the phenazine heterocycle cleanly afforded HP analogues **14** and **15** in 52% and 65% yields, respectively.[28]

To gain further insight into the structure-activity relationships of HP antibacterial agents, we employed multiple routes to generate new analogues for our biological studies. In the first route, we utilized a Wohl-Aue reaction between 4-bromoaniline **45** and 2-nitroanisole **46** which afforded 8-bromo-1-hydroxyphenazine **57** (Supporting Information) in 2% yield after refluxing with potassium hydroxide (KOH) in toluene. Despite this low yield, we were able to advance **57** through the BBr_3 demethylation/dibromination route to afford HP **18** in 45% yield over the final 2 steps (Scheme 1.B). For the second synthetic pathway, we carried out a Suzuki coupling between **35** and *n*-butylboronic acid pinacol ester using 20 mol% tetrakis(triphenylphosphine)palladium(0), followed by subsequent BBr_3 demethylation and NBS bromination reactions to afford lone HP analogue **22** in 17% yield over 3 steps (Scheme 1.C). For the third synthetic route, we employed an *O*-allylation/Claisen rearrangement sequence leading to 2-allylated HP analogues **23** (85% over 3 steps) and **24** (34% over 3 steps) (Scheme 1.D). Finally, we synthesized a small series of halogenated quinoxalines (**25-28**, see Supporting Information for details). Although these diverse synthetic routes have not been exhausted, we were able to make several HP analogues that were critical in probing various positions of the HP scaffold.

Antibacterial Evaluation and HeLa Cytotoxicity Studies.

Our biological investigations were initiated with the screening of our HP-inspired library (including halogenated quinoline **29**) in MIC assays against a panel of pathogenic bacteria, including: *S. aureus*, *S. epidermidis*, *Enterococcus faecium*, *Acinetobacter baumannii*, *Pseudomonas aeruginosa*, *Klebsiella pneumoniae* and *Escherichia coli*. Lead antibacterial agents from these initial studies were then evaluated against *M. tuberculosis* (H37Ra). Several bacterial strains used in this panel were drug-resistant (i.e., MRSA-2, MRSA BAA-44, MRSA BAA-1707, *S. epidermidis* 35984 are methicillin-resistant; *E. faecium* 700221 is vancomycin-resistant; Table 1).

During initial MIC assays, 4,7,8-trihalogenated phenazine **12** proved to be the most potent analogue against methicillin-resistant *S. aureus* (MRSA) planktonic cells by reporting MIC values of 0.15-0.59 μM (Table 1 and

Supporting Table 2 for a panel of five additional MRSA isolates). HP **12** also demonstrated potent antibacterial activity against methicillin-sensitive *S. epidermidis* (MIC = 0.39 μM; ATCC 12228) and methicillin-resistant *S. epidermidis* (MIC = 0.78 μM; MRSE ATCC 35984). This was our first encounter of an active HP analogue that did not possess a bromine atom in the 2-position of the phenazine. Based on this finding, the two chlorine atoms in the 7- and 8-positions of **12** override the previously established structure-activity relationship (SAR) requirements of having a bromine in the 2-position to be an active antibacterial agent. In addition, HP analogues **7**, **8**, **11**, **14** and **18** demonstrated sub-micromolar growth inhibition activities against at least one MRSA strain while **12** and **18** demonstrated this level of antibacterial potency against all three MRSA strains (MIC 0.15-0.78 μM; Table 1). Quinoxaline analogues **25-28** demonstrated a range of antibacterial activities against MRSA strains (MIC 0.78-25 μM, Table 1), with **28** proving to be the most potent quinoxaline analogue. Select HP analogues (**11, 12, 14, 22, 26, 28**; Supporting Table 2) were evaluated against a panel of five additional MRSA isolates and reported potent anti-MRSA activities

HP analogues that had potent antibacterial agents against MRSA strains demonstrated similar antibacterial activities against *S. epidermidis.* Against methicillin-sensitive *S. epidermidis* 12228, we observed a 12- to 15-fold increase in antibacterial potency for halogenated phenazines **14-17** (MIC 0.08-0.10 μM; Table 1) compared to parent HP **2** (MIC 1.17 μM). HP analogues **15**, **16** and **22** (MIC 0.30-0.59 μM) proved to be the most potent antibacterial agents against methicillin-resistant *S. epidermidis* (MRSE 35984).

When evaluated for antibacterial activity against VRE, HPs **14-18** and **22** demonstrated an 8- to 64-fold increase in antibacterial activities (MIC 0.10-0.39 μM) compared to parent HP **2** (MIC = 6.25 μM; 2.2 μg/mL) with **14** proving to be the most potent analogue (MIC = 0.10 μM; 0.05 μg/mL). HP analogues **11** and **12** (MIC 3.13-6.25 μM) demonstrated near equipotent antibacterial activities compared to **2** against VRE, despite demonstrating improvements in antibacterial activities against staphylococcal pathogens. The remaining HP analogues demonstrated antibacterial activities against VRE comparable to parent HP **2** (Table 1).

There is a critical need to identify new antibacterial agents that target the slow-growing pathogen *Mycobacterium tuberculosis* (MtB), which results in 1.5 million deaths each year worldwide.[5,30]

Mycobacterium pathogens are difficult to treat as these persistent bacteria are involved in many chronic and recurring infections,[5,31] similar to bacterial biofilms. We tested a small panel of our most potent HP analogues against *M. tuberculosis* (MtB) H37Ra (ATCC 25177) in MIC assays (Table 1). HP **2** demonstrated moderate antibacterial activity against *M. tuberculosis* with an MIC value of 25 μM. Four halogenated phenazine analogues were identified to be more potent than **2**, including **14** (MIC 12.5 μM), **16** (MIC 6.25 μM) with the most potent analogues **11** and **12** reporting MIC values of 3.13 μM against *M. tuberculosis*. HP analogues **17** and **28** were found to be inactive (MIC > 50 μM) against *M. tuberculosis* in these assays. HPs **11** and **12** demonstrated antibacterial potency against *M. tuberculosis* near that of streptomycin (MIC 1.32 μM; positive control). Select HPs possess impressive antibacterial activities that could be useful in treating life-threatening MtB infections.

Following our investigations with gram-positive pathogens and *M. tuberculosis*, we evaluated 12 HP analogues against gram-negative pathogens, including: *A. baumannii* (ATCC 19606), *P. aeruginosa* (PAO1), *K. pneumoniae* (ATCC 13883) and *E. coli* (UAEC-1, clinical isolate from a bloodstream infection at the University of Arkansas Med. School). Quinoxaline analogue **25** was the only HP analogue to demonstrate good antibacterial activities against the gram-negative pathogens *A. baumannii* 19606 (MIC 6.25 μM) and *E. coli* UAEC-1 (MIC 12.5 μM) with moderate antibacterial activity against *K. pneumoniae* 13883 (MIC 37.5 μM) (Supporting Information). All 12 HP analogues evaluated in this panel, including quinoxaline **25**, proved to be inactive against *P. aeruginosa* (PAO1; MIC > 100 μM).

Select HP analogues were then evaluated for mammalian cytotoxicity in lactate dehydrogenate (LDH) release assays[32] against HeLa cells to determine if HP analogues target bacteria and not mammalian cells, a critical aspect of developing new antibacterial agents (Table 1). In LDH release assays, all 15 HP analogues that were evaluated against HeLa cells demonstrated excellent cytotoxicity profiles with several HP analogues not showing any observable cytotoxicity at 100 μM. Only HP **14** demonstrated cytotoxicity at 100 μM; however, no cytotoxicity was observed for this analogue at 50 μM. Considering the sub-micromolar antibacterial activity of many HP analogues against MRSA, MRSE and VRE, our HeLa cell data demonstrates that HP analogues

demonstrate a very high degree of specificity targeting bacterial cells over mammalian cells, which is promising for this new class of antibacterial agents.

Bacterial Biofilm Eradication and Hemolysis Studies.

Following the initial antibacterial assessment, 24 HP analogues were advanced to biofilm eradication studies against clinical isolate MRSA-2 alongside conventional antibiotics and other controls agents. For biofilm eradication assays, we used the Calgary Biofilm Device (CBD)[33-35] which allows bacterial biofilms to be established on pegs that are anchored to the lid of a 96-well plate and submerged in inoculated media. Pegs (i.e., CBD lid) with established bacterial biofilms are then transferred to a second 96-well plate containing serial dilutions of test compound (i.e., halogenated phenazine, antibiotic) for biofilm eradication. After compound treatment, the CBD pegs are then transferred to a third 96-well plate containing only fresh media to allow any viable biofilms to recover and disperse planktonic cells from the viable biofilm, resulting in turbid wells. Microtiter wells that are not turbid result from eradicated biofilms (the lowest test concentration that results in a lack of turbidity is considered to be a compound's minimal biofilm eradication concentration or MBEC).

Using the CBD assay, we were able to determine the relative killing dynamics for a compound against both planktonic and biofilm cells in a single assay as the CBD assay can also be used to determine minimum bactericidal concentrations from the media in the test plate (MBC; planktonic killing; Table 2). In addition to MRSA-2, we evaluated panels of 8, 7, 18 and 14 HP analogues and various control compounds (i.e., conventional antibiotics) against MRSA BAA-1707, MRSA BAA-44, MRSE 35984 and VRE 700221 biofilms using the CBD assay, respectively (Table 2). We found the CBD assay to be highly robust for these phenotypic screening purposes[28,36] in addition to being useful in quantifying biofilm (persister) cell killing with select compounds from treated and untreated CBD pegs.

Of the 24 HP analogues that were evaluated against MRSA-2, eight analogues demonstrated more potent biofilm-eradicating activity than HP **2** (MBEC = 93.8 μM; Table 2), including: **8**, **11**, **12**, **14**, **15**, **16**, **17** and **18**. Seven of the eight more potent HP analogues contain additional halogen atom substitutions in the 7- and/or 8-positions of the phenazine heterocycle. Several of these HP analogues were then evaluated against BAA-1707

(Figure 3) and BAA-44, all proving to be potent eradicating agents against these MRSA biofilms. HP analogue **14** (2-bromo-7,8-dichloro-4-iodo-1-hydroxyphenazine) reported the most potent activity against MRSA biofilms with MBEC values of 6.25-9.38 μM (i.e., 10- to 60-fold more potent than parent HP **2**) while HP analogues **16-18** also demonstrated potent biofilm-eradicating activities against all MRSA strains (MBEC = 9.38-50 μM). At the MBEC value against MRSA-2, HP **14** eradicates >3-log (>99.9%) of persister cells within the corresponding biofilms (viable biofilm cell count determined from CBD peg; Figure 5).

Front-running antibiotics used to treat MRSA infections (i.e., vancomycin, daptomycin and linezolid) were tested alongside our HP analogues. Vancomycin, daptomycin and linezolid were unable to eradicate MRSA biofilms at the highest test concentrations (MBEC >2,000 μM; Figure 3; Table 2) despite demonstrating moderate to potent planktonic killing in the same experiment (MBC 3.0-125 μM). These results are illustrative of the innate ability of biofilms to tolerate high levels of antibiotics despite having susceptible planktonic counterparts. During these investigations, doxycycline and rifampin were both found to eradicate MRSA-2 biofilms in CBD assays (MBEC = 46.9 μM); however, the MBEC:MBC ratio for these conventional antibiotics is >23 compared to MBEC:MBC ratios of 1-6 for most active HP analogues in the same assays (Table 2).

In addition to conventional antibiotics, select biofilm-eradicating agents and persister cell killing agents were also evaluated in our CBD assays as positive controls to determine the effectiveness of our HP analogues on a head-to-head basis. This panel of known biofilm- or persister-eradicating agents includes: **64** (quaternary ammonium cation-10 or QAC-10; an AMP mimic and membrane-lysing agent),[17] carbonyl cyanide *m*-chlorophenyl hydrazine (CCCP; membrane-active ionophore)[37], *N*-acetyl cysteine (NAC; antioxidant)[38] and pyrazinamide (persister killer).[4,39,40] From this panel of control agents, we found **64** to have the most potent biofilm eradication activities (MBEC = 125 μM) against MRSA-2. CCCP reported weak biofilm eradication activities against MRSA-2 (MBEC = 1,000 μM) while NAC and pyrazinamide did not show any biofilm eradication activities (MBEC > 2,000 μM) using the CBD assay. Compared to our lead HP **14**, this small panel of known biofilm-eradicating agents and persister cell killers were found to be 12- to >200-fold less potent at eradicating MRSA-2 biofilms (Table 2).

From the panel of 18 HP analogues that were evaluated against MRSE biofilms, 13 demonstrated more potent biofilm eradication activities than HP **2** (MBEC = 250 μM; Table 2). As with our MRSA biofilm eradication studies, we found HP **14** to demonstrate unparalleled biofilm-eradicating activities against MRSE (MBEC = 2.35 μM; >100-fold more potent than **2**; Figure 3). At the MBEC values against MRSE, HPs **14** and **16** eradicated >4-log (>99.99%) of persister cells within the corresponding biofilms while demonstrating 1-2 log reduction in viable biofilm cells at sub-MBEC values (viable biofilm cells determined from CBD peg; Figure 4; see **16** in Supporting Information). Several HP analogues (**15**, **16**, **17**, **18**) that possess halogen atoms in the 7- and/or 8-position of the phenazine heterocycle proved to eradicate MRSE biofilms with a high level of potency (MBEC = 3.13-25 μM). In addition, HPs **4** and **22** (non-substituted analogues in the 7- and 8-position) reported MBEC values of 23.5 μM against MRSE biofilms. In these investigations, MRSE biofilms did show some susceptibility to various control compounds (**64**, MBEC = 31.3 μM; CCCP, MBEC = 93.8 μM; rifampin, MBEC = 15.6 μM); however, vancomycin was unable to eradicate MRSE biofilms at the highest concentration tested (MBEC >2,000 μM; Table 2).

VRE biofilms were found to be highly sensitive to several of our HP analogues, including parent HP **2** (MBEC = 9.38 μM, Figure 3). Nine of the 14 HP analogues we tested demonstrated more potency compared to **2**, with 4 HP analogues (**14**, **16-18**) reporting sub-micromolar MBEC values against VRE biofilms (Table 2). HP **14** demonstrated the most potent biofilm eradication activity against VRE biofilms and gave an MBEC value of 0.20 μM (47-fold more potent than **2**). **64** potently eradicates VRE biofilms (MBEC = 3.0 μM) similar to previous reports;[17] however, NAC demonstrates no biofilm eradication activity in our CBD assays, despite a previous report of *E. faecium* biofilm eradication.[38]

In addition to Calgary Biofilm Device experiments, we evaluated select HPs against staphylococcal biofilms in live/dead staining experiments. HP **14** was added to 24 hour old MRSE biofilms at 0.1, 1 and 10 μM and allowed to incubate at 37 °C for an additional 24 hours. Following this, images of the treated and untreated *S. epidermidis* biofilm were taken using fluorescence microscopy (Figure 5). Halogenated phenazine **14** removed all detectable MRSE biofilm cells from the glass surface at 10 μM and a significant amount of the biofilm cells

at 1 μM. Interestingly, at 0.1 μM of **14** a significant amount of MRSE biofilm cells were eradicated, however, not cleared from within the biofilm. We previously observed HPs **12** and **14** to clear MRSA-2 biofilms at sub-micromolar concentrations, well below their corresponding MBEC values in CBD experiments.[28] It appears that halogenated phenazine analogues are able to eradicate bacterial biofilms, in part, due to an effective clearance mechanism.

HP analogues were also evaluated for hemolysis activity against human red blood cells (RBCs; Table 2) at 200 μM to probe if HP analogues operated through a membrane-lysing mechanism, typical of antimicrobial peptides.[17] We found HP analogues do not generally lyse RBCs as only analogues **6** (5%) and **22** (12%) demonstrated low levels of hemolytic activity at 200 μM while the remainder of the HP analogues demonstrated insignificant hemolysis (i.e., < 3%). We found AMP-mimic and known membrane-lysing agent **64** to cause >99% hemolysis of RBCs in these assays alongside our HP analogues. This hemolysis data provides further support that HP analogues preferentially target bacterial cells over mammalian cell types, similar to our observations with HeLa cells.

Structure-Activity Relationships (SAR) and Profiles of Halogenated Phenazine Analogues.

Our focused, yet structurally diverse sub-classes of halogenated phenazines (**2-24**), quinoxalines (**25-28**) and quinoline (**29**) small molecules (Figure 6) provided significant structure-activity relationship details for this subset of potent biofilm-eradicating agents while illuminating interesting biological profiles (Figure 7). Active HP analogues demonstrated good to outstanding gram-positive antibacterial and biofilm eradication activities. In addition, HP analogues demonstrated potent antibacterial activities for select HPs against *M. tuberculosis* (Table 1, Figure 7). Interestingly, all HP analogues were found to be completely inactive against our panel of gram-negative bacteria.

Chlorine atom substitution at the 2- and/or 4-position of **2** resulted in a loss of MRSA-2 biofilm eradication activities (see HP **3**, **5**, **7**, **9**; Figure 6) with the only exception to this trend being HP **6** which demonstrated essentially equipotent biofilm eradication activities compared to **2**. 2,4-Diiodo-1-hydroxyphenazine **4** maintained biofilm eradication activities compared to **2**, while 2-bromo-4-iodo-1-hydroxyphenazine **8** gave a

slight (<2-fold) increase in biofilm eradication activities against MRSA-2. Reversing the mixed halogenated pattern of **8** to afford HP **10** (4-bromo-2-iodo-1-hydroxyphenazine) resulted in a 4-fold reduction in biofilm eradication activity between these two mixed HP analogues.

The 7- and 8-positions of the HP scaffold (i.e., structure **2**) proved to be critical for potent biofilm eradication activities as the introduction of a single bromine atom at the 8-position of HP **18** resulted in a 4-fold increase in biofilm eradication potency against MRSA-2 compared to **2** (Figures 6 & 7). HP **18** also proved to be 10- to 30-fold more potent at eradicating biofilms against our panel of MRSA (BAA-1707 and BAA-44), MRSE and VRE strains compared to **2** (Table 2). Introducing a fourth bromine atom at the 7-position (from HP **18**) corresponds to HP **17**, which resulted in a 2-fold loss of biofilm eradication activity against MRSA-2 compared to **18**. This loss in activity was also observed in the other two MRSA strains (Table 2); however, HP **17** proved to be more potent than **18** against MRSE and VRE biofilms (Figure 7). 7,8-Dichlorohalogenated phenazine analogues **15** and **16** demonstrated equipotent biofilm eradication potencies to HP **17** and **18** against MRSA-2. HP **16** also demonstrated potent biofilm eradication activities against MRSE and VRE that were on pace with **17**. HP analogue **14** is very similar to **16** except the 2-bromine atom is exchanged with a 2-iodide atom, which resulted in a significant increase in biofilm-eradicating potencies across all MRSA, MRSE and VRE strains tested. This single halogen atom difference resulted in a 5-fold increase in potency for HP **14** against MRSA-2 compared to HP **16**, and a 10-fold increase in biofilm eradication activity compared to parent HP **2**. HP **14** demonstrated the most potent biofilm eradication across the entire panel of gram-positive pathogens, corresponding to a 60-fold increase against MRSA BAA-1707, 100-fold increase against MRSE and 47-fold increase in VRE biofilm eradication activities compared to parent HP **2** (Figure 6). Interestingly, dibrominated benzophenazine analogue **19** (containing a fused aromatic ring at the 7- and 8-position of the HP scaffold) did not show any biofilm eradication activities at the highest concentration tested, resulting in a >2- to >20-fold loss in activity compared to active HPs **2** and **14**, respectively (Table 2).

From our previous studies,[26] we determined that the bromine atom in the 2-position of the HP scaffold is crucial for antibacterial activities; however, when the 7- and 8-positions of the HP scaffold are chlorinated, HP

analogues bearing a bromine (**11**) or iodide (**12**) atom in the 4-position without a halogen atom in the 2-position demonstrate potent biofilm eradication activities overriding our previous SAR knowledge of this class of antibacterial agents (Figure 7). Despite HP **11** and **12** being 3-fold more potent than parent HP **2**, these analogues were less active than lead HP **14** against MRSA-2 biofilms (Figure 6). HP **11** and **12** demonstrated moderate eradication activities compared to other HP analogues against MRSE and VRE biofilms. Although HPs **11** and **12** demonstrated a moderate level of biofilm eradication, these analogues were found to possess the most potent antibacterial activities for any HPs evaluated against *M. tuberculosis*. Alternatively, when the two chlorine atoms in the 7- and 8-position of **11** and **12** were replaced with bromine atoms (giving HP **13**), there was a significant loss in activity as no eradication was observed against MRSA, MRSE and VRE biofilms. Removal of the 4-halogen atom of 7,8-dichlorinated analogues **11** and **12** resulted in inactive HP **21**, demonstrating the necessity for the 4-position to be halogenated in this HP sub-series (Figure 7).

We expanded our library to include alkylated HP analogues and we were delighted to discover that 4-butyl HP analogue **22** (mono-brominated only at 2-position) demonstrated potent biofilm eradication activities during these investigations (Figures 6 & 7). Against MRSA-2, HP **22** demonstrated a 2-fold reduction in biofilm eradication activities compared to **2**; however, this trend was reversed as **22** was found to be more potent than **2** against MRSA-1707 (6-fold increase in potency), VRE (5-fold increase in potency) and MRSE (10-fold increase in potency) biofilms. This was the first time that a monohalogenated HP analogue demonstrated biofilm eradication activities and sets the stage for future analogue synthesis. Interestingly, switching the positions of the alkyl and bromine groups results in a complete loss of antibacterial activity (i.e., HPs **23** and **24**).

Simplified HP scaffolds, including quinoxalines **25-28** and quinoline **29**, led to analogues with reduced or no biofilm eradication activities against MRSA-2 (Figures 6 & 7). From the quinoxaline series, unsubstituted halogenated quinoxalines **25** and **26** were inactive as biofilm eradicating agents at the highest concentrations tested, which are >20-fold higher than active concentrations for HP **2**. 2,3-Dimethylquinoxaline analogues gave interesting results with dibrominated analogue **27** demonstrating weak biofilm eradication activities while the

diiodinated analogue **28** was equipotent with HP **2** as a biofilm eradicator against MRSA-2. Halogenated quinoline **29** demonstrated a slight loss in biofilm eradication activities against MRSA-2 compared to **2**; however, **29** is more potent than **2** against MRSE and VRE biofilms. Our group is also developing halogenated quinoline antibacterial and antibiofilm agents as an elaboration of our halogenated phenazine program.[36,41,42]

Preliminary Mechanistic Insights.

Phenazine antibiotics, which include **1**, are class of redox-active metabolites produced by *Pseudomonas* and *Streptomyces* bacteria.[43,44] It has been proposed that the central ring of the phenazine heterocycle undergoes a redox reaction that generates superoxide anions which, in turn, kills various bacteria and fungi.[44] Several active HP analogues were assayed in MIC experiments against MRSA-2 in combination with tiron (1 mM, which is non-toxic to MRSA-2; Table 3), a superoxide quenching agent[45] (*S. epidermidis* 12228 and VRE were also evaluated, see Supporting Information). In these experiments, tiron did not suppress the antibacterial activity of HP analogues despite eliminating the antibacterial activity of 8-hydroxyquinoline (8-HQ; positive control).[28] In analogous experiments with other free radical scavengers, we found that thiourea (500 μM), manganese (III) tetrakis (4-benzoic acid)porphyrin (MnTBAP; 1 mM) or ascorbic acid (1 mM) did not suppress the antibacterial activities of HP **2**. Based on these findings, we conclude that HP analogues do not operate primarily through a redox-based mechanism.

Halogenated quinolines (i.e., **29**) and halogenated phenazines (**2-22**) share several structural features, including a dihalogenated phenolic ring adjacent to the nitrogen atom of a heterocycle. Halogenated quinolines (i.e., 5,7-dihalo-8-hydroxyquinolines) and 8-hydroxyquinolines complex metal(II)-cations allowing an array of diverse bioactivity profiles which have been studied by our group[36,42] and others.[46-49] Biofilm-eradicating HP analogues have a metal-binding moiety that is analogous to 8-hydroxyquinolines where the 1-hydroxyl group and the adjacent phenazine nitrogen atom would form a 5-membered ring upon metal complexation. Recently, Beauvais and co-workers reported that 1-hydroxyphenazine chelates metal ions resulting antifungal activities against *Aspergillus fumigatus* through iron-starvation.[50] Although 1-hydroxyphenazine is inactive against staphylococcal pathogens,[26] this metal-binding moiety is critical to the potent activities of halogenated

phenazines as methylation of the phenolic hydroxyl group in **2** abolishes the antibacterial activity of the HP scaffold.[26]

We co-treated select HP analogues with 200 μM of copper(II), iron(II) and magnesium(II) in MIC assays against MRSA-2 (Table 3) to determine if certain metal(II) cations would complex to HP analogues and eliminate their antibacterial activities. Upon co-treatment with copper(II), HP analogues demonstrated a significant decrease in antibacterial activities (up to 48-fold loss determined by elevated MIC values by copper(II) co-treatment), while iron(II) slightly decreases antibacterial activity (up to 5-fold elevated MIC values) and magnesium(II) had no effect against MRSA-2 (data not shown). We have observed similar activities with halogenated quinoline small molecules.[36,42]

Using UV-Vis spectroscopy, we demonstrated that HP **2** and halogenated quinoline **29** directly bind copper(II) and iron(II) (Figure 8). When treating HP **2** (λ_{max} = 440 nm; Figure 8A) with copper(II), an insoluble complex forms which precipitates out of solution resulting in the disappearance of UV-Vis absorbance. For halogenated quinoline analogue **29** (λ_{max} = 314 nm; Figure 8B) we observed a soluble copper(II)-complex resulting in a shift in absorbance to λ_{max} = 394 nm. We also demonstrate that HP **2** (ligand) binds copper(II) in a 2:1 ligand:copper(II) ratio (see titration curve in Supporting Information), analogous to previous findings with 1-hydroxyphenazine[50] and halogenated quinolines.[46-49] In addition, we demonstrated that HP **2** binds iron(II) resulting in a soluble complex and a concomitant shift in absorbance (λ_{max} = 550 nm; Figure 8C). We felt that metal binding could be influenced by the acidity of the phenolic proton, which we measured experimentally for HPs **2** (pKa = 6.74; most acidic, largest shift in MIC with Cu^{2+}), **11**, **12** (pKa = 7.70; least acidic, smallest shift in MIC with Cu^{2+}) and **14** (Table 3). Although pKa values correlated to changes in MIC with copper(II) co-treatment, changes in MIC values with iron(II) co-treatment had less of a correlation to phenolic acidity of these HP analogues. We then evaluated the general metal-chelating agent ethylenediaminetetraacetic acid (EDTA) in biofilm eradication assays against MRSA-2 to determine if metal sequestration was critical to the observed biofilm eradication activities observed by our HP analogues; however, EDTA demonstrated no biofilm eradication at the highest concentrations tested (MBEC > 2,000 μM).

Interestingly, in kill curve experiments against bacteria in exponential-growth phase, our HP analogues demonstrated bacteriostatic activity as the minimum bactericidal concentration (MBC) is >4-fold higher than corresponding MIC values (see Supporting Information). At higher concentrations, we previously demonstrated that **14** slowly kills stationary MRSA-2 cells unlike **64**, which is a rapid killer of stationary MRSA cells.[28] From these results, we conclude that HP analogues operate primarily through a unique metal(II)-dependent mechanism that is critical to persister cells in biofilms; however, detailed mechanistic investigations are required to fully understand our preliminary findings.

CONCLUSION

Here, we described the chemical synthesis, biological investigations and detailed structure-activity relationships of a new series of HP analogues, inspired by marine phenazine antibiotic **1**. Halogenated phenazines demonstrate potent biofilm eradication activities against multiple MRSA, MRSE and VRE biofilms and operate through a non-membrane lysing mechanism, similar to antimicrobial peptide mimics. HP **14** proved to be the most potent biofilm-eradicating agent against every drug-resistant isolate tested for biofilm eradication and killed >99.9% of MRSA and MRSE persister cells at the corresponding MBEC value. In addition, HPs **11** and **12** demonstrated potent antibacterial activity against the slow-growing human pathogen *M. tuberculosis* (MIC = 3.13 μM; ~1 μg/mL). We demonstrated that HP **2** directly binds copper(II) and iron(II), which likely plays a role in the mode of action; however, detailed mechanistic studies are required. Halogenated phenazines are a promising class of biofilm-eradicating agents that effectively target multiple persistent bacterial phenotypes (i.e., biofilms, slow-growing MtB) and could lead to novel therapeutics to treat a spectrum of chronic and recurring bacterial infections.

EXPERIMENTAL SECTION

General Information. All synthetic reactions were carried out under an inert atmosphere of argon unless otherwise specified. Reagents for chemical synthesis were purchased from commercial sources and used without further purification. All microwave reactions were carried out in an Anton Paar Monowave 300 Microwave Synthesis Reactor. Analytical thin layer chromatography (TLC) was performed using 250 μm

Silica Gel 60 F254 pre-coated plates (EMD Chemicals Inc.). Flash column chromatography was performed using 230-400 Mesh 60Å Silica Gel from Sorbent Technologies. All melting points were obtained, uncorrected, using a Mel-Temp capillary melting point apparatus from Laboratory Services, Inc. NMR experiments were recorded using broadband probes on a Varian Mercury-Plus-400 spectrometer via VNMR-J software (400 MHz for ^{1}H and 100 MHz for ^{13}C). Spectra for all new compounds were obtained in the following solvents (reference peaks also included for ^{1}H and ^{13}C NMRs): $CDCl_3$ (^{1}H NMR: 7.26 ppm; ^{13}C NMR: 77.23 ppm), d_6-DMSO (^{1}H NMR: 2.50 ppm; ^{13}C NMR: 39.52 ppm) and d_4-MeOD (^{1}H NMR: 3.31 ppm; ^{13}C NMR: 49.00 ppm). ^{1}H NMR multiplicities are reported as: s = singlet, br. s = broad singlet, d = doublet, t = triplet, q = quartet, m = multiplet. High-Resolution Mass Spectrometry (HRMS) were obtained for all new compounds from the Chemistry Department at the University of Florida. The purities of all compounds evaluated in biological assays were confirmed to be ≥95% by LC-MS using a Shimadzu Prominence HPLC system, AB Sciex 3200 QTRAP spectrometer, and a Kinetex C18 column (50 mm × 2.1 mm × 2.6 μm) with a 13 minute linear gradient from 10-80% acetonitrile in 0.1% formic acid at a flow rate of 0.25 mL/min.

Bacterial strains used during these investigations include: methicillin-resistant *Staphylococcus aureus* (Clinical Isolate from Shands Hospital in Gainesville, FL: MRSA-2; ATCC strains: BAA-1707, BAA-44) methicillin-resistant *Staphylococcus epidermidis* (MRSE strain ATCC 35984; methicillin-sensitive strain ATCC 12228), vancomycin-resistant *Enterococcus faecium* (VRE strain ATCC 700221), *Acinetobacter baumannii* (ATCC 19606), *Pseudomonas aeruginosa* (PAO1), *Klebsiella pneumoniae* (ATCC 13883) and *Escherichia coli* clinical isolate (UAEC-1). All compounds were stored as DMSO stocks at room temperature in the absence of light for several months at a time without observing any loss in biological activity. To ensure compound integrity of our DMSO stock solutions, we did not subject DMSO stocks of our test compounds to freeze-thaw cycles.

Chemistry.

General dihalogenation procedure at the 2- and 4-position of the phenazine ring (3, 18): 8-Bromo-1-hydroxyphenazine **57** (43.2 mg, 0.16 mmol) and *N*-bromosuccinimide, (57.5 mg, 0.32 mmol) were dissolved in dichloromethane (10 mL) and allowed to stir at room temperature for 2 hours. The reaction contents were then

concentrated, adsorbed onto silica gel and purified via column chromatography using dichloromethane to elute **18** as a dark orange solid (46%, 31.3 mg). **Note:** Analogous reaction conditions were used to synthesize analogue **3**.

2,4-Dichloro-1-hydroxyphenazine **(3)**: 47% yield; yellow solid. ^{1}H NMR (400 MHz, $CDCl_3$): δ 8.40 (m, 1H), 8.36 (br. s, 1H), 8.26 (m, 1H), 7.96-7.89 (m, 2H), 7.91 (s, 1H). ^{13}C NMR (100 MHz, $CDCl_3$): δ 147.0, 143.9, 141.7, 139.0, 134.6, 132.3, 132.0, 131.9, 130.4, 129.1, 123.2, 114.6. HRMS (DART): calc. for $C_{12}H_7N_2Cl_2O$ $[M+H]^+$: 264.9930, found: 264.9932. MP: 205 - 207 °C.

2,4,8-Tribromo-1-hydroxyphenazine **(18)**: 46% yield; orange solid. ^{1}H NMR (400 MHz, d_6-DMSO): δ 8.50 (d, J = 2.2 Hz, 1H), 8.45 (s, 1H), 8.26 (d, J = 9.3 Hz, 1H), 8.15 (dd, J = 9.3, 2.2 Hz, 1H). ^{13}C NMR (100 MHz, d_6-DMSO): δ 150.9, 141.5, 141.5, 139.6, 137.3, 135.8, 135.3, 131.3, 130.6, 125.7, 111.6, 105.3. HRMS (ESI): calc. for $C_{12}H_6Br_3N_2O$ $[M+H]^+$: 430.8025, found: 430.8010. MP: 239 - 241 °C.

Synthesis of 2,4,-Diiodo-1-hydroxyphenazine (4): To a mixture of 1-hydroxyphenazine **42** (68.1 mg, 0.35 mmol) in a 9:1 solution of glacial acetic acid:water (15 mL) was added sodium chloride (244 mg, 4.17 mmol), sodium periodate (446 mg, 2.08 mmol), then potassium iodide (241 mg, 2.08 mmol). The reaction was then allowed to stir at room temperature for 8 hours. Upon completion of this reaction (as determined by TLC analysis using dichloromethane), the reaction contents were transferred to a separatory funnel containing a solution of saturated sodium bicarbonate, and the aqueous layer was extracted with dichloromethane. The organic layer was collected, dried with anhydrous sodium sulfate and concentrated *in vacuo*. The resulting solid was adsorbed onto silica gel (dry loading with dichloromethane) and purified via column chromatography using first hexanes to elute an undesired purple product, followed by dichloromethane to elute pure **4** (19%, 79.2 mg), which was isolated as a yellow solid. ^{1}H NMR (400 MHz, $CDCl_3$): δ 8.78 (br. s, 1H), 8.65 (s, 1H), 8.40 (m, 1H), 8.27 (m, 1H), 7.97 – 7.88 (m, 2H). ^{13}C NMR (100 MHz, $CDCl_3$): δ 153.9, 148.1, 144.9, 142.3, 141.7, 133.1, 132.1, 131.8, 130.3, 128.9, 89.6, 76.5. HRMS (DART): calc. for $C_{12}H_7I_2N_2O$ $[M+H]^+$: 448.8642, found: 448.8623. MP: 193 - 195 °C.

General procedure for the monohalogenation at the 2-position of the phenazine ring (5-10, 15 and 22): 4-Chloro-1-hydroxyphenazine **40** (75.4 mg, 0.33 mmol) and *N*-bromosuccinimide (58.2 mg, 0.33 mmol) were

dissolved in 15 mL dichloromethane and allowed to stir at room temperature for 1 hour. The reaction contents were then concentrated, adsorbed onto silica gel and purified via column chromatography using dichloromethane to elute 2-bromo-4-chloro-1-hydroxyphenazine **7**, which was isolated as a yellow solid (91%, 91.9 mg). **Note:** Analogous procedures were used for chlorination and iodination using *N*-chlorosuccinimide and *N*-iodosuccinimide, respectively.

4-Bromo-2-chloro-1-hydroxyphenazine **(5)**: 34% yield; yellow solid. ^{1}H NMR (400 MHz, $CDCl_3$): δ 8.44 – 8.35 (m, 2H), 8.26 (m, 1H), 8.13 (s, 1H), 7.96 – 7.89 (m, 2H). ^{13}C NMR (100 MHz, $CDCl_3$): δ 147.6, 144.2, 141.6, 139.7, 135.4, 134.6, 132.3, 131.8, 130.4, 128.9, 115.2, 112.9. HRMS (DART): calc. for $C_{12}H_7BrClN_2O$ $[M+H]^+$: 308.9425, found: 308.9437. MP: 229 - 231 °C.

2-Chloro-4-iodo-1-hydroxyphenazine **(6)**: 42% yield; yellow solid. ^{1}H NMR (400 MHz, $CDCl_3$): δ 8.43 (br. s, 1H), 8.39 (m, 1H), 8.38 (s, 1H), 8.26 (m, 1H), 7.96 – 7.89 (m, 2H). ^{13}C NMR (100 MHz, $CDCl_3$): δ 148.5, 144.6, 141.9, 141.7, 141.3, 134.0, 132.2, 131.7, 130.3, 128.8, 116.0, 88.9. HRMS (DART): calc. for $C_{12}H_7ClIN_2O$ $[M+H]^+$: 356.9286, found: 356.9281. MP: 183 - 185 °C.

2-Bromo-4-chloro-1-hydroxyphenazine **(7)**: 91% yield; yellow solid. ^{1}H NMR (400 MHz, $CDCl_3$): δ 8.47 (br. s, 1H), 8.39 (m, 1H), 8.25 (m, 1H), 8.03 (s, 1H), 7.99 - 7.86 (m, 2H). ^{13}C NMR (100 MHz, $CDCl_3$): δ 148.6, 144.0, 141.6, 139.4, 134.4, 134.0, 132.3, 131.9, 130.5, 129.1, 123.4, 102.6. HRMS (DART): calc. for $C_{12}H_7BrClN_2O$ $[M+H]^+$: 308.9425, found: 308.9434. MP: 212 - 214 °C.

2-Bromo-4-iodo-1-hydroxyphenazine **(8)**: 65% yield; yellow solid. ^{1}H NMR (400 MHz, $CDCl_3$): δ 8.57 (br. s, 1H), 8.51 (s, 1H), 8.40 (m, 1H), 8.27 (m, 1H), 7.97 - 7.89 (m, 2H). ^{13}C NMR (100 MHz, $CDCl_3$): δ 150.2, 144.7, 143.8, 141.7, 141.7, 134.0, 132.2, 131.8, 130.3, 128.8, 104.2, 89.2. HRMS (DART): calc. for $C_{12}H_7BrIN_2O$ $[M+H]^+$: 400.8781, found: 400.8785. MP: 186 - 188 °C.

4-Chloro-2-iodo-1-hydroxyphenazine **(9)**: 82% yield; yellow solid. ^{1}H NMR (400 MHz, $CDCl_3$): δ 8.67 (br. s, 1H), 8.36 (m, 1H), 8.21 (m, 1H), 8.14 (s, 1H), 7.98 - 7.85 (m, 2H). ^{13}C NMR (100 MHz, $CDCl_3$): δ 152.2,

144.1, 141.4, 139.8, 138.4, 133.3, 132.2, 131.9, 130.4, 129.1, 123.4, 74.4. HRMS (DART): calc. for $C_{12}H_7ClIN_2O$ $[M+H]^+$: 356.9286, found: 356.9299. MP: 175 - 177 °C.

4-Bromo-2-iodo-1-hydroxyphenazine **(10)**: 48% yield; yellow solid. ^{1}H NMR (400 MHz, $CDCl_3$): δ 8.71 (br. s, 1H), 8.36 (m, 1H), 8.35 (s, 1H), 8.22 (m, 1H), 7.95 - 7.87 (m, 2H). ^{13}C NMR (100 MHz, $CDCl_3$): δ 152.8, 144.4, 141.7, 141.4, 140.6, 133.4, 132.2, 131.9, 130.3, 129.0, 113.3, 75.2. HRMS (DART): calc. for $C_{12}H_7BrIN_2O$ $[M+H]^+$: 400.8781, found: 400.8770. MP: 188 - 190 °C.

4,7,8-Tribromo-2-chloro-1-hydroxyphenazine **(15)**: 65% yield; orange solid. ^{1}H NMR (400 MHz, d_6-DMSO): δ 8.78 (s, 1H), 8.68 (s, 1H), 8.41 (s, 1H). ^{13}C NMR (100 MHz, d_6-DMSO): δ 149.5, 141.7, 140.4, 139.7, 136.3, 135.9, 133.3, 132.6, 128.2, 128.1, 116.5, 111.3. HRMS (DART): calc. for $C_{12}H_5Br_3ClN_2O$ $[M+H]^+$: 464.7635, found: 464.7614. MP: 242 - 244 °C.

2-Bromo-4-butyl-1-hydroxyphenazine **(22)**: 53% yield; yellow solid. ^{1}H NMR (400 MHz, $CDCl_3$): δ 8.38 (br. s, 1H), 8.28 (m, 1H), 8.21 (m, 1H), 7.90 – 7.80 (m, 2H), 7.67 (t, J = 0.8 Hz 1H), 3.26 (dt, J = 7.8, 0.9 Hz, 2H), 1.83 – 1.75 (m, 2H), 1.47 (tq, J = 7.4, 7.4 Hz, 2H), 0.99 (t, J = 7.4 Hz, 3H). ^{13}C NMR (100 MHz, $CDCl_3$): δ 147.2, 143.4, 142.0, 141.0, 134.7, 134.0, 132.9, 131.2, 130.6, 130.5, 129.0, 103.5, 32.9, 30.1, 22.9, 14.3. HRMS (ESI): calc. for $C_{16}H_{16}BrN_2O$ $[M+H]^+$: 331.0441, found: 331.0462. MP: 135 - 137 °C.

General procedure for boron tribromide demethylation (13, 40, 41, 43, 57, 58): To a round bottom flask was added 7,8-dichloro-1-methoxyphenazine **20** (218 mg, 0.78 mmol) dissolved in anhydrous dichloromethane (18 mL). The mixture was brought to -78 °C in a dry ice bath before dropwise addition of 1M boron tribromide solution in dichloromethane (5.5 mL, 5.5 mmol). The reaction was left to stir at -78 °C for 1 hour, and then allowed to reach ambient temperature for reaction overnight. The reaction was heated to reflux for 8 hours until complete (monitored by TLC). The solution was transferred to a separatory funnel containing an aqueous solution of saturated sodium bicarbonate, and then extracted with dichloromethane. Organic solvents were dried with sodium sulfate, filtered through cotton, and removed *in vacuo*. The resulting solid was purified via column chromatography using dichloromethane to elute compound **21** as an orange solid (>99%, 209 mg). Note: Analogous procedures were used for all demethylation reactions using BBr_3.

4,7,8-Tribromo-1-hydroxyphenazine **(13)**: 96% yield; orange solid. ^{1}H NMR (400 MHz, $CDCl_3$): δ 8.80 (s, 1H), 8.62 (s, 1H), 8.12 (d, *J* = 8.1 Hz, 1H), 8.04 (s, 1H), 7.18 (d, *J* = 8.1 Hz, 1H). ^{13}C NMR (100 MHz, $CDCl_3$): δ 151.8, 143.2, 141.4, 140.2, 135.8, 135.6, 134.0, 132.7, 129.7, 129.1, 112.5, 110.7. HRMS (DART): calc. for $C_{12}H_6Br_3N_2O$ $[M+H]^+$: 430.8025, found: 430.8017. MP: >260 °C.

4-Chloro-1-hydroxyphenazine **(40)**: 95% yield; yellow solid. ^{1}H NMR (400 MHz, $CDCl_3$): δ 8.40 (m, 1H), 8.23 (m, 1H), 8.17 (s, 1H), 7.97 – 7.86 (m, 2H), 7.87 (d, *J* = 8.2 Hz, 1H), 7.17 (d, *J* = 8.2 Hz, 1H). ^{13}C NMR (100 MHz, $CDCl_3$): δ 151.1, 144.2, 141.4, 140.3, 135.1, 131.6, 131.1, 130.4, 129.1, 122.5, 108.8. Note: One ^{13}C signal missing, likely due to overlap. HRMS (DART): calc. for $C_{12}H_8ClN_2O$ $[M+H]^+$: 231.0320, found: 231.0330. MP: 196 - 198 °C.

4-Iodo-1-hydroxyphenazine **(41)**: 86% yield; yellow solid. ^{1}H NMR (400 MHz, $CDCl_3$): δ 8.41 (m, 1H), 8.36 (d, *J* = 8.0 Hz, 1H), 8.30 – 8.20 (m, 2H), 7.97 – 7.82 (m, 2H), 7.06 (d, *J* = 8.0 Hz, 1H). ^{13}C NMR (100 MHz, $CDCl_3$): δ 152.9, 144.9, 142.6, 141.6, 141.5, 134.9, 131.5, 131.5, 130.2, 128.9, 110.8, 88.4. HRMS (DART): calc. for $C_{12}H_8IN_2O$ $[M+H]^+$: 322.9676, found: 322.9689. MP: 193 - 195 °C.

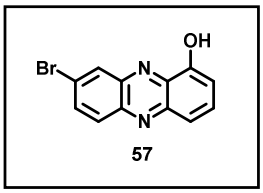

57

8-Bromo-1-hydroxyphenazine **(57)**: >99% yield; yellow solid. ^{1}H NMR (400 MHz, $CDCl_3$): δ 8.42 (dd, *J* = 2.2, 0.5 Hz, 1H), 8.12 (dd, *J* = 9.2, 0.5 Hz, 1H), 8.09 (s, 1H), 7.90 (dd, *J* = 9.3, 2.2 Hz, 1H), 7.82 – 7.66 (m, 2H), 7.26 (dd, *J* = 6.9, 1.7 Hz, 1H). ^{13}C NMR (100 MHz, $CDCl_3$): δ 151.8, 144.0, 142.9, 141.5, 135.0, 134.7, 132.5, 131.3, 131.1, 125.2, 120.2, 109.9. HRMS (ESI): calc. for $C_{12}H_8BrN_2O$ $[M+H]^+$: 274.9815, found: 274.9826. MP: 189 - 191 °C., lit. 176 - 177 °C.[51]

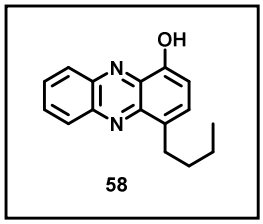

58

4-Butyl-1-hydroxyphenazine **(58)**: 90% yield; 33.2 mg of 58 was isolated as a yellow solid. ^{1}H NMR (400 MHz, $CDCl_3$): δ 8.28 (m, 1H), 8.17 (m, 1H), 8.10 (br. s, 1H), 7.84 – 7.76 (m, 2H), 7.53 (dt, *J* = 7.5, 0.9 Hz, 1H), 7.15 (d, *J* = 7.5 Hz, 1H), 3.28 (td, *J* = 7.4 Hz, 0.9 Hz, 2H), 1.84 – 1.75 (m, 2H), 1.47 (tq, *J* = 7.4, 7.4 Hz, 2H), 0.99 (t, *J* = 7.4 Hz, 3H). ^{13}C NMR (100 MHz, $CDCl_3$): δ 149.7, 143.5, 142.9, 140.8, 135.0, 132.6, 130.4, 130.4, 130.2, 129.6, 129.1, 108.7, 33.0, 30.3, 22.9, 14.3. HRMS (ESI): calc. for $C_{16}H_{17}N_2O$ $[M+H]^+$: 253.1335, found: 253.1325. MP: 138 - 140 °C.

General procedure for the halogenation of the 4-position to synthesize 23 and 24: 2-Allyl-1-hydroxyphenazine **62** (46.5 mg, 0.20 mmol) and *N*-bromosuccinimide (35.1 mg, 0.20 mmol) were dissolved in 10 mL dichloromethane and allowed to stir at room temperature for 1 hour. The reaction contents were then concentrated, adsorbed onto silica gel and purified via column chromatography using dichloromethane to elute 2-allyl-4-bromo-1-hydroxyphenazine **23**, which was isolated as a yellow solid (93%, 58.8 mg). **Note:** An analogous procedure was used to synthesize **24**.

2-Allyl-4-bromo-1-hydroxyphenazine **(23)**: 93%% yield; yellow solid. ^{1}H NMR (400 MHz, $CDCl_3$): δ 8.35 (m, 1H), 8.22 (s, 1H), 8.16 (m, 1H), 7.98 (s, 1H), 7.92 – 7.76 (m, 2H), 6.06 (ddt, *J* = 16.7, 10.1, 6.6 Hz, 1H), 5.21 (ddt, *J* = 16.7, 1.7, 1.6 Hz, 1H), 5.17 (ddt, *J* = 10.1, 1.7, 1.5 Hz, 1H) 3.66 (ddd, *J* = 6.6, 1.6, 1.5 Hz, 2H). ^{13}C NMR (100 MHz, $CDCl_3$): δ 148.2, 144.0, 141.4, 140.0, 136.9, 135.4, 134.8, 131.3, 131.0, 130.3, 128.9, 121.8, 117.1, 112.0, 33.8. HRMS (ESI): calc. for $C_{15}H_{12}BrN_2O$ $[M+H]^+$: 315.0128, found: 315.0127. MP: 149 - 151 °C.

2-Allyl-4,7,8-tribromo-1-hydroxyphenazine **(24)**: 39% yield; yellow solid. ^{1}H NMR (400 MHz, $CDCl_3$): δ 8.74 (s, 1H), 8.57 (s, 1H), 8.07 (br. s, 1H), 8.03 (s, 1H), 6.04 (ddt, *J* = 16.8, 10.1, 6.6 Hz, 1H), 5.21 (dd, 16.8, 1.6 Hz, 1H), 5.19 (dd, 10.1, 1.6 Hz, 1H), 3.66 (d, *J* = 6.6 Hz, 2H). ^{13}C NMR (100 MHz, $CDCl_3$): δ 148.2, 142.7, 140.4, 140.2, 138.1, 135.3, 135.0, 134.0, 132.6, 128.9, 128.5, 123.1, 117.5, 112.2, 33.8. HRMS (ESI): calc. for $C_{15}H_{14}Br_3N_2O$ $[M+H]^+$: 472.8318, found: 472.8331. MP: 187 - 189 °C.

General procedure for monohalogenation at the 4-position of the phenazine (33, 36, 38): 7,8-Dichloro-1-methoxyphenazine **20** (151 mg, 0.54 mmol) was dissolved in dichloromethane (15 mL) before *N*-

bromosuccinimide (106 mg, 0.60 mmol) was added and the reaction was brought to reflux. The mixture was left to stir overnight until complete (monitored by TLC with dichloromethane). At this time, the reaction was concentrated and adsorbed onto silica gel (via dissolving the crude reaction contents and silica gel in dichloromethane, then concentrating via rotavap) and purified via column chromatography using dichloromethane to elute pure 4-bromo-7,8-dichloro-1-methoxyphenazine **36**, which was isolated as a dark yellow solid (96%, 185.2 mg). **Notes:** Analogous procedures were used for the chlorination and iodination of 1-methoxyphenazines using *N*-chlorosuccinimide or *N*-iodosuccinimide.

4-Chloro-1-methoxyphenazine **(33)**: 76% yield; yellow solid. ^{1}H NMR (400 MHz, $CDCl_3$): δ 8.19 – 8.08 (m, 2H), 7.71 – 7.61 (m, 2H), 7.53 (d, *J* = 8.2 Hz, 1H), 6.66 (d, *J* = 8.2 Hz, 1H), 3.90 (s, 3H). ^{13}C NMR (100 MHz, $CDCl_3$): δ 154.0, 142.9, 141.8, 139.9, 136.6, 131.1, 130.8, 129.6, 129.5, 129.2, 123.5, 105.7, 56.3. HRMS (DART): calc. for $C_{13}H_{10}ClN_2O$ $[M+H]^+$: 245.0476, found: 245.0484. MP: 149 - 151 °C.

4-Bromo-7,8-dichloro-1-methoxyphenazine **(36)**: 96% yield; yellow solid. ^{1}H NMR (400 MHz, $CDCl_3$): δ 8.56 (s, 1H), 8.54 (s, 1H), 8.11 (d, *J* = 8.3 Hz, 1H), 6.99 (d, *J* = 8.3 Hz, 1H), 4.17 (s, 3H). ^{13}C NMR (100 MHz, $CDCl_3$): δ 155.3, 142.2, 141.6, 140.9, 137.8, 136.8, 136.4, 134.4, 130.2, 130.2, 114.3, 107.9, 57.0. HRMS (DART): calc. for $C_{13}H_8BrCl_2N_2O$ $[M+H]^+$: 356.9192, found: 356.9194. MP: 199 - 201 °C.

4,7,8-Tribromo-1-methoxyphenazine **(38)**: 86% yield; yellow solid. ^{1}H NMR (400 MHz, $CDCl_3$): δ 8.75 (s, 1H), 8.72 (s, 1H), 8.10 (d, *J* = 8.3 Hz, 1H), 6.98 (d, *J* = 8.3 Hz, 1H), 4.16 (s, 3H). ^{13}C NMR (100 MHz, $CDCl_3$): δ 155.3, 142.5, 141.6, 141.2, 137.8, 134.5, 133.7, 133.6, 129.1, 128.6, 114.4, 107.9, 57.0. HRMS (DART): calc. for $C_{13}H_8Br_3N_2O$ $[M+H]^+$: 444.8181, found: 444.8181. MP: 241 - 243 °C.

Synthesis of 4-iodo-1-methoxyphenazine 35 (potassium iodide and sodium periodate): To a mixture of 1-methoxyphenazine **32** (356 mg, 1.69 mmol) in 9:1 acetic acid:water (30 mL) was added sodium chloride (435 mg, 7.45 mmol), sodium periodate (869 mg, 4.06 mmol), then potassium iodide (675 mg, 4.06 mmol). The reaction was heated to 65 °C and allowed to stir for 21 hours. After completion of this reaction as determined by TLC analysis (with dichloromethane), the reaction mixture was washed with a saturated solution of sodium bicarbonate and then partitioned with dichloromethane. The organic layers were then collected, dried with

anhydrous sodium sulfate and concentrated *in vacuo*. The resulting solid was then dry loaded onto silica gel (using dichloromethane) and purified via column chromatography using first hexanes to elute purple side product, followed by dichloromethane to elute **35** as a yellow solid (68%, 388.0 mg). ^{1}H NMR (400 MHz, $CDCl_3$): δ 8.37 (m, 1H), 8.32 (m, 1H), 8.30 (d, *J* = 8.2 Hz, 1H), 7.89 – 7.79 (m, 2H), 6.81 (d, *J* = 8.2 Hz, 1H), 4.12 (s, 3H). ^{13}C NMR (100 MHz, $CDCl_3$): δ 156.2, 144.1, 142.6, 140.2, 136.9, 131.4, 131.1, 129.8, 129.7, 108.2, 91.0, 56.8. Note: One signal obscured likely due to overlap. HRMS (DART): calc. for $C_{13}H_{10}IN_2O$ $[M+H]^+$: 336.9832, found: 336.9829. MP: 169 - 171 °C.

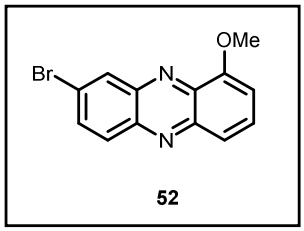

52

Synthesis of 7-bromo-1-methoxyphenazine (52): To a 100 mL round-bottom flask was added 4-bromoaniline **45** (1.74 mL, 14.2 mmol), 2-nitroanisole **46** (2.45 g, 14.2 mmol), and potassium hydroxide (3.99 g, 71.1 mmol) in toluene (20 mL). The reaction was then allowed to reflux for 24 hours. After the reaction was complete, the reaction contents were allowed to cool to room temperature. The reaction mixture was transferred to a separatory funnel, partitioned between ethyl acetate, and then washed with water and brine. The organic layers were collected, dried with anhydrous sodium sulfate, filtered and then concentrated *in vacuo*. The resulting crude solid was purified via column chromatography using 99:1 to 85:15 hexanes:ethyl acetate to afford **52**, which was isolated as a yellow solid (2%, 87.7 mg). ^{1}H NMR (400 MHz, $CDCl_3$): δ 8.58 (d, *J* = 2.2 Hz, 1H), 8.05 (d, *J* = 9.2 Hz, 1H), 7.86 (dd, *J* = 9.2, 2.2 Hz, 1H), 7.80 – 7.70 (m, 2H), 7.05 (dd, *J* = 7.1, 1.5 Hz, 1H), 4.15 (s, 3H). ^{13}C NMR (100 MHz, $CDCl_3$): δ 155.2, 144.4, 142.5, 142.2, 137.2, 134.7, 132.3, 131.1, 130.8, 124.7, 121.6, 107.3, 56.7. HRMS (ESI): calc. for $C_{13}H_{10}BrN_2O$ $[M+H]^+$: 288.9971, found: 288.9960. MP: 194 - 196 °C., lit. 187 - 188 °C.[51]

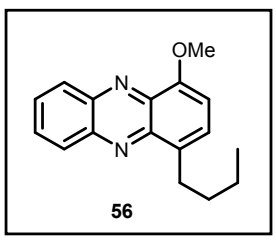

56

Synthesis of 4-butyl-1-methoxyphenazine (56): To a 50 mL round-bottom flask was added 4-iodomethoxyphenazine **35** (146 mg, 0.43 mmol), tetrakis(triphenylphosphine)palladium(0) (100 mg, 0.1 mmol), sodium hydroxide (347 mg, 8.67 mmol), and *n*-butylboronic acid pinacol ester **64** (1.43 mL, 6.72 mmol) in a 2:1 solution of toluene:water (6 mL). The mixture was heated to 90 °C in an oil bath and left to stir for 48 hours. After cooling to room temperature, the reaction mixture was transferred to a separatory funnel, partitioned between an aqueous solution of saturated sodium bicarbonate and ethyl acetate. The resulting organic layer was washed with a 1 N solution of hydrochloric acid, and then brine. The organic layers were combined and dried with anhydrous sodium sulfate and concentrated *in vacuo*. The resulting crude material was purified via column chromatography using 99:1 to 85:15 hexanes:ethyl acetate to afford **56** as a yellow solid (34% yield, 38.9 mg). ^{1}H NMR (400 MHz, $CDCl_3$): δ 8.38 (m, 1H), 8.26 (m, 1H), 7.85 – 7.78 (m, 2H), 7.54 (dt, *J* = 7.8, 0.9 Hz, 1H), 7.00 (d, *J* = 7.8 Hz, 1H), 4.15 (s, 3H), 3.30 (td, *J* = 7.6, 0.9 Hz, 2H), 1.87 – 1.72 (m, 2H), 1.47 (tq, *J* = 7.4, 7.4 Hz, 2H), 0.99 (t, *J* = 7.4 Hz, 3H). ^{13}C NMR (100 MHz, $CDCl_3$): δ 153.4, 143.3, 143.0, 141.9, 137.2, 133.9, 130.4, 130.2, 130.1, 130.1, 128.4, 106.5, 56.5, 32.9, 30.6, 22.9, 14.3. HRMS (ESI): calc. for $C_{17}H_{19}N_2O$ $[M+H]^+$: 267.1492, found: 267.1497. MP: 77 - 79 °C.

General procedure for phenolic allylation (60, 61): Potassium carbonate (866 mg, 6.27 mmol) was added to a stirring solution of 1-hydroxyphenazine **42** (247 mg, 1.25 mmol) in 15 mL acetone. The resulting mixture was allowed to stir at room temperature for 30 minutes before allyl bromide (0.13 mL, 1.51 mmol) was added to the reaction. The resulting reaction mixture was allowed to stir for an additional 17 hours at reflux. The reaction contents were then transferred to a separatory funnel and extracted with ethyl acetate. The organic contents were then dried with anhydrous sodium sulfate and then removed *in vacuo*. The resulting crude solid was purified via column chromatography using 99:1 to 90:10 hexanes:ethyl acetate to afford 1-allyloxyphenazines **60**, which was isolated as a yellow solid (85%, 251.0 mg). **Note:** An analogous procedure was used to synthesize **61**.

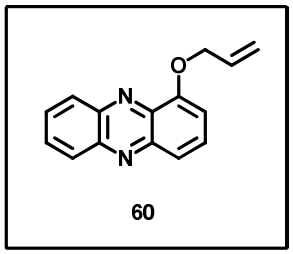

60

1-(Allyloxy)phenazine **(60)**: 85% yield; yellow solid. ^{1}H NMR (100 MHz, $CDCl_3$): δ 8.33 (m, 1H), 8.15 (m, 1H), 7.79 – 7.70 (m, 3H), 7.63 (dd, *J* = 8.9, 7.6 Hz, 1H), 6.99 (d, *J* = 7.6 Hz, 1H), 6.17 (ddt, *J* = 17.3, 10.6, 5.5 Hz, 1H), 5.47 (ddt, *J* = 17.3, 1.6, 1.6 Hz, 1H), 5.32 (ddt, *J* = 10.6, 1.6, 1.6 Hz, 1H), 4.88 (ddd, *J* = 5.5, 1.6, 1.6 Hz, 2H). ^{13}C NMR (100 MHz, $CDCl_3$): δ 154.0, 144.3, 143.5, 142.3, 137.1, 132.7, 130.8, 130.4, 130.4, 130.1, 129.3, 121.6, 118.6, 108.2, 70.2. HRMS (ESI): calc. for $C_{15}H_{13}N_2O$ $[M+H]^+$: 237.1022, found: 237.1026. MP: 117 - 119 °C.

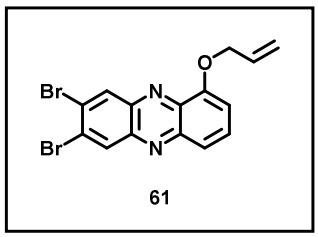

61

7,8-Dibromo-1-allyloxyphenazine **(61)**: 88% yield; orange solid. ^{1}H NMR (400 MHz, $CDCl_3$): δ 8.70 (s, 1H), 8.51 (s, 1H), 7.76 – 7.69 (m, 2H), 7.07 (dd, *J* = 5.9, 2.8 Hz, 1H), 6.21 (ddt, *J* = 17.4, 10.6, 5.4 Hz, 1H), 5.53 (ddt, *J* = 17.4, 1.5, 1.5 Hz, 1H), 5.39 (ddt, *J* = 10.6, 1.5, 1.3 Hz, 1H), 4.92 (ddd, *J* = 5.4, 1.5, 1.3 Hz, 2H). ^{13}C NMR (100 MHz, $CDCl_3$): δ 154.2, 144.8, 142.4, 141.2, 137.6, 134.1, 133.2, 132.6, 131.7, 128.0, 127.2, 121.7, 119.0, 109.1, 70.4. HRMS (ESI): calc. for $C_{15}H_{10}Br_2N_2O$ $[M+H]^+$: 394.9213, found: 394.9211. MP: 170 - 172 °C.

General procedure for Claisen rearrangement (62, 63): To an 8 mL sealed microwave vial was added 1-(allyloxy)phenazine **60** (19.4 mg, 0.08 mmol) in ethanol (4 mL). The resulting mixture was then heated at 150 °C in the microwave reactor for 90 minutes. The solvent was removed *in vacuo* and the resulting solid was purified via column chromatography using dichloromethane to elute, affording 2-allylphenazine **62**, which was

isolated as a yellow solid (>99%, 19.3 mg). **Note:** Analogous reaction conditions were used to synthesize **63** from **61**.

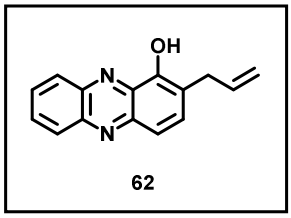

62

2-Allyl-1-hydroxyphenazine **(62)**: >99% yield; yellow solid. ^{1}H NMR (100 MHz, $CDCl_3$): δ 8.28 (br. s, 1H), 8.21 (m, 1H), 8.13 (m, 1H), 7.81 – 7.74 (m, 2H), 7.72 (d, *J* = 9.1 Hz, 1H), 7.64 (d, *J* = 9.1 Hz, 1H), 6.09 (ddt, *J* = 16.7, 10.1, 6.6 Hz, 1H), 5.18 (ddt, *J* = 16.7, 1.7, 1.7 Hz, 1H), 5.14 (ddt, *J* = 10.1, 1.7 Hz, 1.6 Hz, 1H) 3.68 (ddd, *J* = 6.7, 1.7, 1.6 Hz, 2H). ^{13}C NMR (100 MHz, $CDCl_3$): δ 148.2, 143.8, 143.0, 141.3, 136.0, 134.6, 134.5, 130.4, 130.4, 129.9, 129.2, 120.8, 119.6, 116.5, 34.0. HRMS (ESI): calc. for $C_{15}H_{13}N_2O$ $[M+H]^+$: 237.1022, found: 237.1017. MP: 112 - 114 °C.

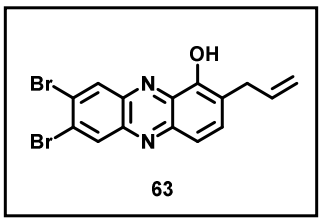

63

2-Allyl-7,8-dibromo-1-hydroxyphenazine **(63)**: >99% yield; orange solid. ^{1}H NMR (400 MHz, $CDCl_3$): δ 8.59 (d, *J* = 0.4 Hz, 1H), 8.56 (d, *J* = 0.4 Hz, 1H), 8.07 (s, 1H), 7.74 – 7.69 (m, 2H), 6.07 (ddt, *J* = 17.1, 10.1, 6.6 Hz, 1H), 5.19 (ddt, *J* = 17.1, 1.6, 1.6 Hz, 1H), 5.16 (ddt, *J* = 10.1, 1.6, 1.5 Hz, 1H) 3.69 (ddd, *J* = 6.6, 1.6, 1.5 Hz, 2H). ^{13}C NMR (100 MHz, $CDCl_3$): δ 148.3, 143.5, 142.7, 140.2, 135.7, 135.6, 135.0, 133.7, 133.0, 127.7, 127.6, 122.2, 119.9, 116.8, 34.1. HRMS (ESI): calc. for $C_{15}H_{10}Br_2N_2O$ $[M+H]^+$: 394.9213, found: 394.9216. MP: 199 - 201 °C.

Biology.

Microdilution Minimum Inhibitory Concentration (MIC) Assay. The minimum inhibitory concentration (MIC) for each compound was determined by the broth microdilution method as recommended by the Clinical and Laboratory Standards Institute (CLSI).[52] In a 96-well plate, eleven two-fold serial dilutions of each compound were made in a final volume of 100 μL Luria Broth. Each well was inoculated with ~10^5 bacterial

cells at the initial time of incubation, prepared from a fresh log phase culture (OD_{600} of 0.5 to 1.0 depending on bacterial strain). The MIC was defined as the lowest concentration of compound that prevented bacterial growth after incubating 16 to 18 hours at 37 °C (MIC values were supported by spectrophotometric readings at OD_{600}). The concentration range tested for each phenazine analogue/antibacterial during this study was 0.10 to 100 μM. DMSO served as our vehicle and negative control in each microdilution MIC assay. DMSO was serially diluted with a top concentration of 1% v/v. All compounds were tested in two independent experiments, active compounds were tested in a third independent experiment (lead compounds were tested in more assays as positive controls during these studies).

Microdilution MIC Assay for *Mycobacterium tuberculosis*. *M. tuberculosis* H37Ra (ATCC 25177) was inoculated in 10 mL Middlebrook 7H9 medium and allowed to grow for two weeks. The culture was then diluted with fresh medium until an OD_{600} of 0.01 was reached. Aliquots of 200 μL were then added to each well of a 96-well plate starting from the second column. Test compounds were dissolved in DMSO at final concentration of 10 mM. 7.5 μL of each compound along with DMSO (negative control) and streptomycin (positive control-40mg/ml stock solution) were added to 1.5 mL of the Mycobacterium diluted cultures, resulting in 50 μM final concentration of each halogenated phenazine analogues and 340 μM for streptomycin. The final DMSO concentration was maintained at 0.5%. Aliquots of 400 μL were added to wells of the first column of the 96-well plate and serially diluted two-fold (200 μL) per well across the plate to obtain final concentrations that ranges from 0.024 to 50 μM for the test compounds and 0.16 to 340 μM for streptomycin. Three rows were reserved for each compound. The plates were then incubated at 37°C for seven days. Minimum inhibitory concentrations are reported as the lowest concentration at which no bacterial growth was observed. OD_{600} absorbance was recorded using SpectraMax M5 (Molecular Devices). Data obtained from three independent experiments were analyzed using Excel.

Calgary Biofilm Device (CBD) Experiments. Biofilm eradication experiments were performed using the Calgary Biofilm Device to determine MBC/MBEC values for various compounds of interest (Innovotech, product code: 19111). The Calgary device (96-well plate with lid containing pegs to establish biofilms on) was inoculated with 125 μL of a mid-log phase culture diluted 1,000-fold in tryptic soy broth with 0.5% glucose

(TSBG) to establish bacterial biofilms after incubation at 37 °C for 24 hours. The lid of the Calgary device was then removed, washed and transferred to another 96-well plate containing 2-fold serial dilutions of the test compounds (the "challenge plate"). The total volume of media with compound in each well in the challenge plate is 150 μL. The Calgary device was then incubated at 37 °C for 24 hours. The lid was then removed from the challenge plate and MBC/MBEC values were determined using different final assays. *To determine MBC values*, 20 μL of the challenge plate was transferred into a fresh 96-well plate containing 180 μL TSBG and incubated overnight at 37 °C. The MBC values were determined as the concentration giving a lack of visible bacterial growth (i.e., turbidity). *For the determination of MBEC values*, the Calgary device lid (with attached pegs/treated biofilms) was transferred to a new 96-well plate containing 150 μL of fresh TSBG media in each well and incubated for 24 hours at 37 °C to allow viable biofilms to grow and disperse resulting in turbidity after the incubation period. MBEC values were determined as the lowest test concentration that resulted in eradicated biofilm (i.e., wells that had no turbidity after final incubation period). In select experiments, pegs from the Calgary device were removed from lead biofilm eradicators after final incubation, sonicated for 30 minutes in PBS and plated out to determine biofilm cell killing of lead biofilm-eradicating agents (i.e., colony forming unit per milliliter, CFU/mL; Figure 4). All compounds were tested in two independent experiments, active compounds were tested in a third independent experiment (lead compounds were tested in more assays as positive controls during these studies). Antibiotic controls have been tested in a minimum of three independent experiments. **Note:** MRSA-2, *S. aureus* (ATCC strains: BAA-1707, BAA-44), *S. epidermidis* (ATCC 35984) and VRE (ATCC 700221) were tested using these assay parameters.

Live/Dead staining (Fluorescence Microscopy) of MRSE 35984 biofilms. A mid-log culture of MRSE 35894 was diluted 1:1,000-fold and 500 μL was transferred to each compartment of a 4 compartment CELLview dish (Greiner Bio-One 627871). The dish was then incubated for 24 hours at 37 °C. After this time, the cultures were removed and the plate was washed with 0.9% saline. The dish was then treated with the compounds in fresh media at various concentrations. DMSO was used as our negative control in this assay. The dish was incubated with the compound for 24 hours at 37 °C. After this time, the cultures were removed and the dish was washed with 0.9% saline for 2 minutes. Saline was then removed and 500 μL of the stain (Live/Dead

BacLight Viability Kit, Invitrogen) were added for 15 minutes and left in the dark. After this time, the stain was removed and the dish was washed twice with 0.9% saline. Then the dish was fixed with 500 μL 4% paraformaldehyde in PBS for 30 minutes. Images of remaining MRSE biofilms were then taken with a fluorescence microscope. All data were analyzed using Image J software.

Hemolysis Assay with Red Blood Cells. Freshly drawn human red blood cells (hRBC with ethylenediaminetetraacetic acid (EDTA) as an anticoagulant) were washed with Tris-buffered saline (0.01M Tris-base, 0.155 M sodium chloride (NaCl), pH 7.2) and centrifuged for 5 minutes at 3,500 rpm. The washing was repeated three times with the buffer. In 96-well plate, test were added to the buffer from DMSO stocks. Then 2% hRBCs (50 μL) in buffer were added to test compounds to give a final concentration of 200 μM. The plate was then incubated for 1 hour at 37 °C. After incubation, the plate was centrifuged for 5 minutes at 3,500 rpm. Then 80 μL of the supernatant was transferred to another 96-well plate and the optical density (OD) was read at 405 nm. DMSO served as our negative control (0% hemolysis) while Triton X served as our positive control (100% hemolysis). The percent of hemolysis was calculated as (OD_{405} of the compound- OD_{405} DMSO) / (OD_{405} Triton X- OD_{405} buffer).

LDH Release Assay for HeLa Cytotoxicity Assessment. HeLa cytotoxicity was assessed using the LDH release assay described by CytoTox96 (Promega G1780). HeLa cells were grown in Dulbecco's Modified Eagle Medium (DMEM; Gibco) supplemented with 10% Fetal Bovine Serum (FBS) at 37°C with 5% CO_2. When the HeLa cultures exhibited 70-80% confluence, halogenated phenazines were then diluted by DMEM (10% FBS) at concentrations of 25, 50 and 100 μM and added to HeLa cells. Triton X-100 (at 2% v/v) was used as the positive control for maximum lactate dehydrogenate (LDH) activity in this assay (i.e., complete cell death) while "medium only" lanes served as negative control lanes (i.e., no cell death). DMSO was used as our vehicle control. HeLa cells were treated with compounds for 24 hours and then 50 μL of the supernatant was transferred into a fresh 96-well plate where 50 μL of the reaction mixture was added to the 96-well plate and incubated at room temperature for 30 minutes. Finally, Stop Solution (50 μL) was added to the incubating plates and the absorbance was measured at 490 nm.

HP 2 and 29 Complex Formation with Cu(II) and Fe(II). The rates of phenazine-metal(II) and quinoline-metal(II) complex formation were independently evaluated via UV-vis spectrometry following addition of 0.5 equivalents $CuSO_4$ or Ammonium iron(II) sulfate hexahydrate to stirring solutions of HP **2** or **29** (10 mM, 20 mL) in dimethyl sulfoxide. Spectral scanning was performed from 200 to 900 nm in 2 nm increments. The λ_{max} values were determined to be 440 nm and 314 nm for **2** and **29** respectively. The disappearance of each complex was observed over the indicated time points. Although the copper(II) complex of **29** yielded an easily discernable UV-vis spectrum (λ_{max} = 394 nm), the phenazine-copper complex formation yielded a loss in absorbance due to precipitation. Due to the insolubility of the phenazine:copper complex, the stoichiometry was determined by spectrophotometrically quantifying the concentration of free phenazine in solution following incubation with varying equivalents of $CuSO_4$ (Supporting Figure 1; Supporting Information). Each data point was evaluated in independent experiments wherein 10 mM solutions of HP **2** in methanol (15 mL) were stirred with $CuSO_4$ for 2 hours at room temperature. After this time, the mixtures were filtered and the solvent was removed *in vacuo* to afford free HP **2** as a solid. HP **2** solid was then dissolved in 15 mL of dimethyl sulfoxide and the absorbance at 440 nm was evaluated after a single ten-fold dilution was made. The concentrations of free HP **2** in solution could thus be determined from a calibration curve of serial dilutions of HP **2** in dimethyl sulfoxide (Supporting Figure 2). This data demonstrates >99% of HP **2** (ligand) is bound to copper(II) at a minimum of 2:1 ligand:copper ratio, suggesting the stoichiometry of the ligand:metal complex is 2:1.

ASSOCIATED CONTENT

Supporting Information. Additional information detailing synthetic procedures, biological assays, supporting results, biological images of select assays and NMR spectra for all new compounds can be found in the associated Supporting Information documentation. This material is available free of charge via the Internet at http://pubs.acs.org.

AUTHOR INFORMATION

Corresponding Author.

*E-mail: rhuigens@cop.ufl.edu. Phone: (352) 273-7718.

ACKNOWLEDGMENTS

We would like to acknowledge the University of Florida for start-up funds and for an Opportunity Seed Fund awarded to RWH and SJ. ATG and VMN are University of Florida Graduate Fellows. Images for the graphical abstract associated with this manuscript were provided by the NIH (Courtesy: National Institute of Allergy and Infectious Diseases).

ABBREVIATIONS USED

CBD calgary biofilm device; HP halogenated phenazine; HQ halogenated quinoline; MBEC minimum biofilm eradication concentration; UAEC-1 University of Arkansas *Escherichia coli* isolate-1

REFERENCES

1. Donlan, R. M.; Costerton, J. W. Biofilms: survival mechanisms of clinically relevant microorganisms. *Clin. Microbiol. Rev.* **2002**, *15*, 167-193.
2. Hall-Stoodley, L.; Costerton, J. W.; Stoodley, P. Bacterial biofilms: from the natural environment to infectious diseases. *Nat. Rev. Microbiol.* **2004**, *2*, 95-108.
3. Lewis, K. Persister cells, dormancy and infectious disease. *Nature Rev. Microbiol.* **2007**, *5*, 48-56.
4. Wood, T. K. Combatting bacterial persister cells. *Biotechnol. Bioengineer.* **2016**, *113*, 476-483.
5. Young, D. B.; Perkins, M. D.; Duncan, K.; Barry, C. E. Confronting the scientific obstacles to global control of tuberculosis. *J. Clin. Invest.* **2008**, *118*, 1255-1265.
6. Lewis, K. Persister cells. *Annu. Rev. Microbiol.* **2010**, *64*, 357-372.
7. Conlon, B. P. *Staphylococcus aureus* chronic and relapsing infections: evidence of a role for persister cells. *Bioessays* **2014**, *36*, 991-996.
8. Balaban, N. Q.; Merrin, J.; Chait, R.; Kowalik, L.; Leibler, S. Bacterial persistence as a phenotype switch. *Science* **2004**, *305*, 1622-1625.
9. Wood, T. K.; Knabel, S. J.; Kwan, B. W. Bacterial persister cell formation and dormancy. *Appl. Environ. Microbiol.* **2013**, *79*, 7116-7121.

10. Wolcott, R.; Dowd, S. The role of biofilms: are we hitting the right target? *Plast. Reconstr. Surg.* **2011**, *127*, Suppl. 1: 28S-35S.

11. Worthington, R. J.: Richards, J. J.; Melander, C. Small molecule control of bacterial biofilms. *Org. Biomol. Chem.* **2012**, *10*, 7457-7474.

12. Harbarth, S.; Theuretzbacher, U.; Hackett, J. Antibiotic research and development: business as usual? *J. Antimicrob. Chemother.* **2015**, *70*, 1604-1607.

13. Brackman, G.; Coenye, T. Quorum sensing inhibitors as anti-biofilms agents. *Curr. Pharm. Design* **2015**, *21*, 5-11.

14. De Zoysa, G. H.; Cameron, A. J.; Hegde, V. V.; Raghothama, S.; Sarojini, V. Antimicrobial peptides with potential for biofilm eradication: synthesis and structure activity relationship studies of battacin peptides. *J. Med. Chem.* **2015**, *58*, 625-639.

15. Hoque, J.; Konai, M. M.; Gonuguntla, S.; Manjunath, G. B.; Samaddar, S.; Yarlagadda, V.; Haldar, J. Membrane active small molecules show selective broad spectrum antibacterial activity with no detectable resistance and eradicate biofilms. *J. Med. Chem.* **2015**, *58*, 5486-5500.

16. Hoque, J.; Konai, M. M.; Samaddar, S.; Gonuguntla, S.; Manjunath, G. B.; Ghosh, C.; Haldar, J. Selective and broad spectrum amphiphilic small molecules to combat bacterial resistance and eradicate biofilms. *Chem. Commun.* **2015**, *51*, 13670-13673.

17. Jennings, M. C.; Ator, L. E.; Paniak, T. J.; Minibole, K. P. C., Wuest, W. M. Biofilm eradicating properties of quaternary ammonium amphiphiles: simple mimics of antimicrobial peptides. *ChemBioChem.* **2014**, *15*, 2211-2215.

18. Mitchell, M. A.; Iannetta, A. A.; Jennings, M. C.; Fletcher, M. H.; Wuest, W. M.; Minbiole, K. P. C. Scaffold-hopping of multicationic amphiphiles yields three new classes of antimicrobials. *ChemBioChem.* **2015**, *16*, 2299-2303.

19. Hughes, C. C.; Fenical, W. Antibacterials from the sea. *Chem. Eur. J.* **2010**, *16*, 12512-12525.

20. Ng, W.-L.; Bassler, B. L. Bacterial quorum-sensing network architectures. *Annu. Rev. Genet.* **2009**, *43*, 197-222.

21. Hentzer, M.; Wu, H.; Andersen, J. B.; Riedel, K.; Rasmussen, T. B.; Bagge, N.; Kumar, N.; Schembri, M. A.; Song, Z.; Kristoffersen, P.; Manefield, M.; Costerton, J. W.; Molin, S.; Eberl, L.; Steinberg, P.; Kjelleberg, S.; Høiby, N.; Givskov, M. Attenuation of *Pseudomonas aeruginosa* virulence by quorum sensing inhibitors. *EMBO J.* **2003**, *22*, 3803-3815.

22. Wu, H.; Song, Z.; Hentzer, M.; Andersen, J. B.; Molin, S.; Givskov, M.; Høiby, N. Synthetic furanones inhibit quorum-sensing and enhance bacterial clearance in *Pseudomonas aeruginosa* lung infection in mice. *J. Antimicrob. Chemother.* **2004**, *53*, 1054-1061.

23. Kwan, J. C.; Meickle, T.; Ladwa, D.; Teplitski, M.; Paul, V. J.; Luesch, H. Lyngbyoic acid, a "tagged" fatty acid from a marine cyanobacterium, disrupts quorum sensing in *Pseudomonas aeruginosa*. *Mol. BioSyst.* **2011**, *7*, 1205-1216.

24. Navarro, G.; Cheng, A. T.; Peach, K. C.; Bray, W. M.; Bernan, V. S.; Yildiz, F. H.; Linington, R. G. Image-based 384-well high-throughput screening method for the discovery of skyllamycins A to C as biofilm inhibitors and inducers of biofilm detachment in *Pseudomonas aeruginosa*. *Antimicrob. Agents Chemother.* **2014**, *58*, 1092-1099.

25. Conda-Sheridan, M.; Marler, L.; Park, E. J.; Kondratyuk, T. P.; Jermihov, K.; Mesecar, A. D.; Pezzuto, J. M.; Asolkar, R. N.; Fenical, W.; Cushman, M. Potential chemopreventive agents based on the structure of the lead compound 2-bromo-1-hydroxyphenazine, isolated from *Streptomyces* species, strain CNS284. *J. Med. Chem.* **2010**, *53*, 8688-8699.

26. Borrero, N. V.; Bai, F.; Perez, C.; Duong, B. Q.; Rocca, J. R.; Jin, S.; Huigens III, R. W. Phenazine antibiotic inspired discovery of potent bromophenazine antibacterial agents against *Staphylococcus aureus* and *Staphylococcus epidermidis*. *Org. Biomol. Chem.* **2014**, *12*, 881-886.

27. Garrison, A. T.; Bai, F.; Abouelhassan, Y.; Paciaroni, N. G.; Jin, S.; Huigens III, R.W. Bromophenazine derivatives with potent inhibition, dispersion and eradication activities against *Staphylococcus aureus* biofilms. *RSC Adv.* **2015**, *5*, 1120-1124.

28. Garrison, A. T.; Abouelhassan, Y.; Kallifidas, D.; Bai, F.; Ukhanova, M.; Mai, V.; Jin, S.; Luesch, H.; Huigens III, R. W. Halogenated phenazines that potently eradicate biofilms, MRSA persister cells in

non-biofilm cultures, and *Mycobacterium tuberculosis*. *Angew. Chemie., Int. Ed.* **2015**, *54*, 14819-14823.

29. Pachter, I. J.; Kloetzel, M. C. The Wohl-Aue reaction. I. Structure of benzo [a] phenazine oxides and syntheses of 1,6-dimethoxyphenazine and 1,6-dichlorophenazine. *J. Am. Chem. Soc.* **1951**, *73*, 4958-4961.
30. Evangelopoulos, D.; McHugh, T. D. Improving the tuberculosis drug development pipeline. *Chem. Biol. Drug Des.* **2015**, *86*, 951-960.
31. Pérez-Lago, L.; Navarro, Y.; Montilla, P.; Comas, I.; Herranz, M.; Rodríguez-Gallego, C.; Ruiz Serrano, M. J.; Bouza, E.; García de Viedma, D. Persistent infection by a *Mycobacterium tuberculosis* strain that was theorized to have advantageous properties, as it was responsible for a massive outbreak. *J. Clin. Microbiol.* **2015**, *53*, 3423-3429.
32. Weidmann, E.; Brieger, J.; Jahn, B.; Hoelzer, D.; Bergmann, L.; Mitrou, P. S. Lactate dehydrogenase-release assay: A reliable, nonradioactive technique for analysis of cytotoxic lymphocyte-mediated lytic activity against blasts from acute myelocytic leukemia. *Annu. Hematol.* **1995**, *70*, 153-158.
33. Ceri, H.; Olson, M. E.; Stremick, C.; Read, R. R.; Morck, D.; Buret, A. The calgary biofilm device: new technology for rapid determination of antibiotic susceptibilities of bacterial biofilms. *J. Clin. Microbiol.* **1999**, *37*, 1771-1776.
34. Harrison, J. J.; Turner, R. J.; Joo, D. A.; Stan, M. A.; Chan, C. S.; Allan, N. D.; Vrionis, H. A.; Olson, M. E.; Ceri, H. Copper and quaternary ammonium cations exert synergistic bactericidal and antibiofilm activity against *Pseudomonas aeruginosa*. *Antimicrob. Agents Chemother.* **2008**, *52*, 2870-2881.
35. Harrison, J. J.; Stremick, C. A.; Turner, R. J.; Allan, N. D.; Olson, M. E.; Ceri, H. Microtiter susceptibility testing of microbes growing on peg lids: a miniaturized biofilm model for high-throughput screening. *Nat. Protoc.* **2010**, *5*, 1236-1254.
36. Basak, A.; Abouelhassan, Y.; Huigens III, R. W. Halogenated quinolines discovered through reductive amination with potent eradication activities against MRSA, MRSE and VRE biofilms. *Org. Biomol. Chem.* **2015**, *13*, 10290-10294.

37. Eun, Y. J.; Foss, M. H.; Kiekebusch, D.; Pauw, D. A.; Westler, W. M.; Thanbichler, M.; Weibel, D. B. DCAP: a broad-spectrum antibiotic that targets the cytoplasmic membrane of bacteria. *J. Am. Chem. Soc.* **2012**, *134*, 11322-11325.

38. Quah, S. Y.; Wu, S.; Lui, J. N.; Sum, C. P.; Tan, K. S. *N*-acetylcysteine inhibits growth and eradicates biofilm of *Enterococcus faecalis*. *J. Endod.* **2012**, *38*, 81-85.

39. McCune, R. M.; Feldmann, F. M.; McDermott, W. Microbial persistence. II. Characteristics of the sterile state of tubercle bacilli. *J. Exp. Med.* **1966**, *123*, 469-486.

40. Shi, W.; Zhang, X.; Jiang, X.; Yuan, H.; Lee, J. S.; Barry, C. E.; Wang, H.; Zhang, W.; Zhang, Y. Pyrazinamide inhibits trans-translation in *Mycobacterium tuberculosis*. *Science* **2011**, *333*, 1630-1632.

41. Abouelhassan, Y.; Garrison, A. T.; Burch, G. M.; Wong, W.; Norwood IV, V. M.; Huigens III, R. W. Discovery of quinoline small molecules with potent dispersal activity against methicillin-resistant *Staphylococcus aureus* and *Staphylococcus epidermidis* biofilms using a scaffold hopping strategy. *Bioorg. Med. Chem. Lett.* **2014**, *24*, 5076-5080.

42. Abouelhassan, Y.; Garrison, A. T.; Bai, F.; Norwood IV, V. M.; Nguyen, M.; Jin, S.; Huigens III, R. W. A phytochemical-halogenated quinoline combination therapy strategy for the treatment of pathogenic bacteria. *ChemMedChem* **2015**, *10*, 1157-1162.

43. Laursen, J. B.; Nielsen, J. Phenazine natural products: biosynthesis, synthetic analogues, and biological activity. *Chem. Rev.* **2004**, *104*, 1663-1685.

44. Price-Whelan, A.; Dietrich, L. E. P.; Newman, D. K. Rethinking 'secondary' metabolism: physiological roles for phenazine antibiotics. *Nat. Chem. Biol.* **2006**, *2*, 71-78.

45. Taiwo, F. A. Mechanism of tiron as scavenger of superoxide ions and free electrons. *Spectroscopy* **2008**, *22*, 491-498.

46. Gershon, H.; Parmegiani, R. Antimicrobial activity of 8-quinolinol, its salts with salicylic acid and 3-hydroxy-2-naphthoic acid, and the respective copper (II) chelates in liquid culture. *Appl. Environ. Microbiol.* **1963**, *11*, 62-65.

47. Deraeve, C.; Pitié, M.; Mazarguil, H.; Meunier, B. Bis-8-hydroxyquinoline ligands as potential anti-Alzheimer agents. *New J. Chem.* **2007**, *31*, 193-195.

48. Prachayasittikul, V.; Prachayasittikul, S.; Ruchirawat, S.; Prachayasittikul, V. 8-Hydroxyquinolines: a review of their metal chelating properties and medicinal applications. *Drug Des. Devel. Ther.* **2013**, *7*, 1157-1178.

49. Di Varia, M.; Bazzicalupi, C.; Orioli, P.; Messori, L.; Bruni, B.; Zatta, P. Clioquinol, a drug for Alzheimer's disease specifically interfering with brain metal metabolism: structural characterization of its zinc(II) and copper(II) complexes. *Inorg. Chem.* **2004**, *43*, 3795-3797.

50. Briard, B.; Bomme, P.; Lechner, B. E.; Mislin, G. L. A.; Liar, V.; Prévost, M. C.; Latgé, J. P.; Haas, H.; Beauvais, A. *Pseudomonas aeruginosa* manipulates redox and iron homeostasis of its microbiota partner *Aspergillus fumigatus* via phenazines. *Sci. Rep.* **2015**, *5*; doi:10.1038/srep08220.

51. Chernetskii, V. P.; Kiprianov, A. I. Synthesis of halogen derivatives of phenazine. IV. Bromophenazines. *Zhurnal Obshchei Khimii* **1956**, *26*, 3032-3036.

52. Clinical and Laboratory Standards Institute. **2009**. *Methods for dilution antimicrobial susceptibility tests for bacteria that grow aerobically; approved standard, 8th edition (M7-M8)*, Clinical and Laboratory Standard, Wayne, PA, **2009**.

Figures:

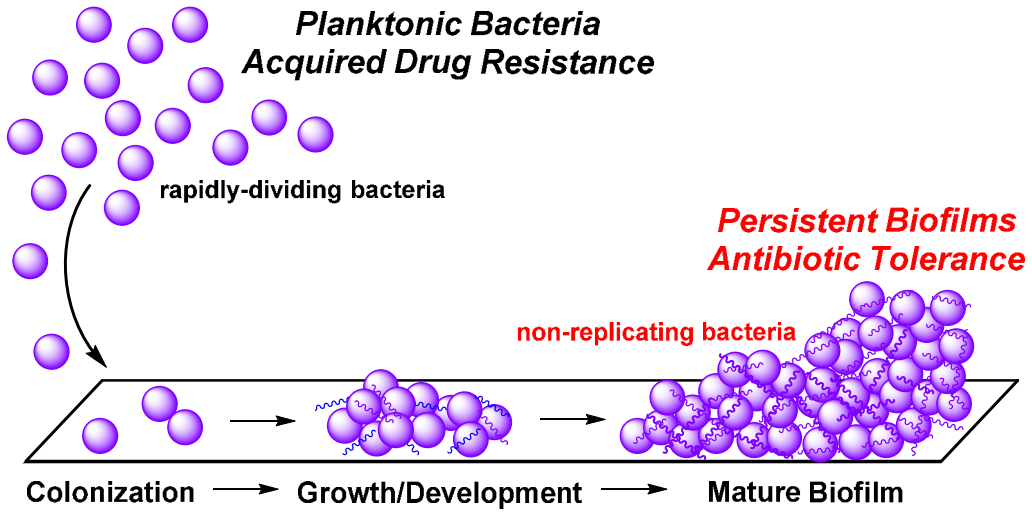

Figure 1. Planktonic bacterial cells are rapidly-dividing and prone to developing antibiotic resistance compared to surface-attached biofilm cells, which are innately tolerant of antibiotic therapies due to their non-replicating phenotype.

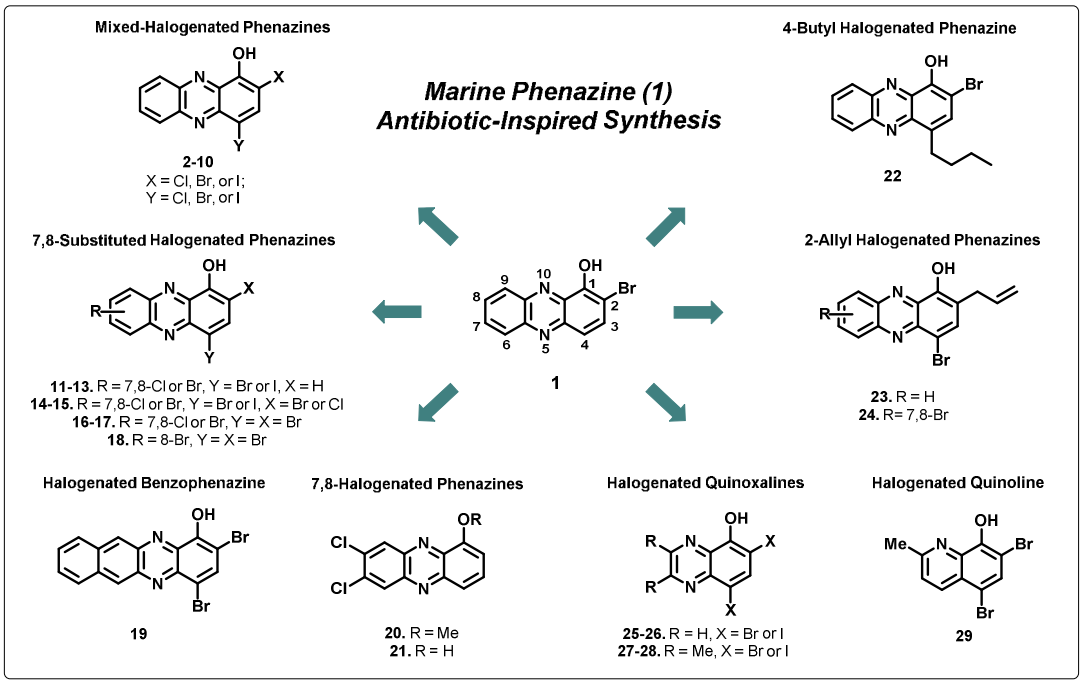

Figure 2. Synthetic analogues of marine phenazine antibiotic (**1**) that were evaluated during these investigations.

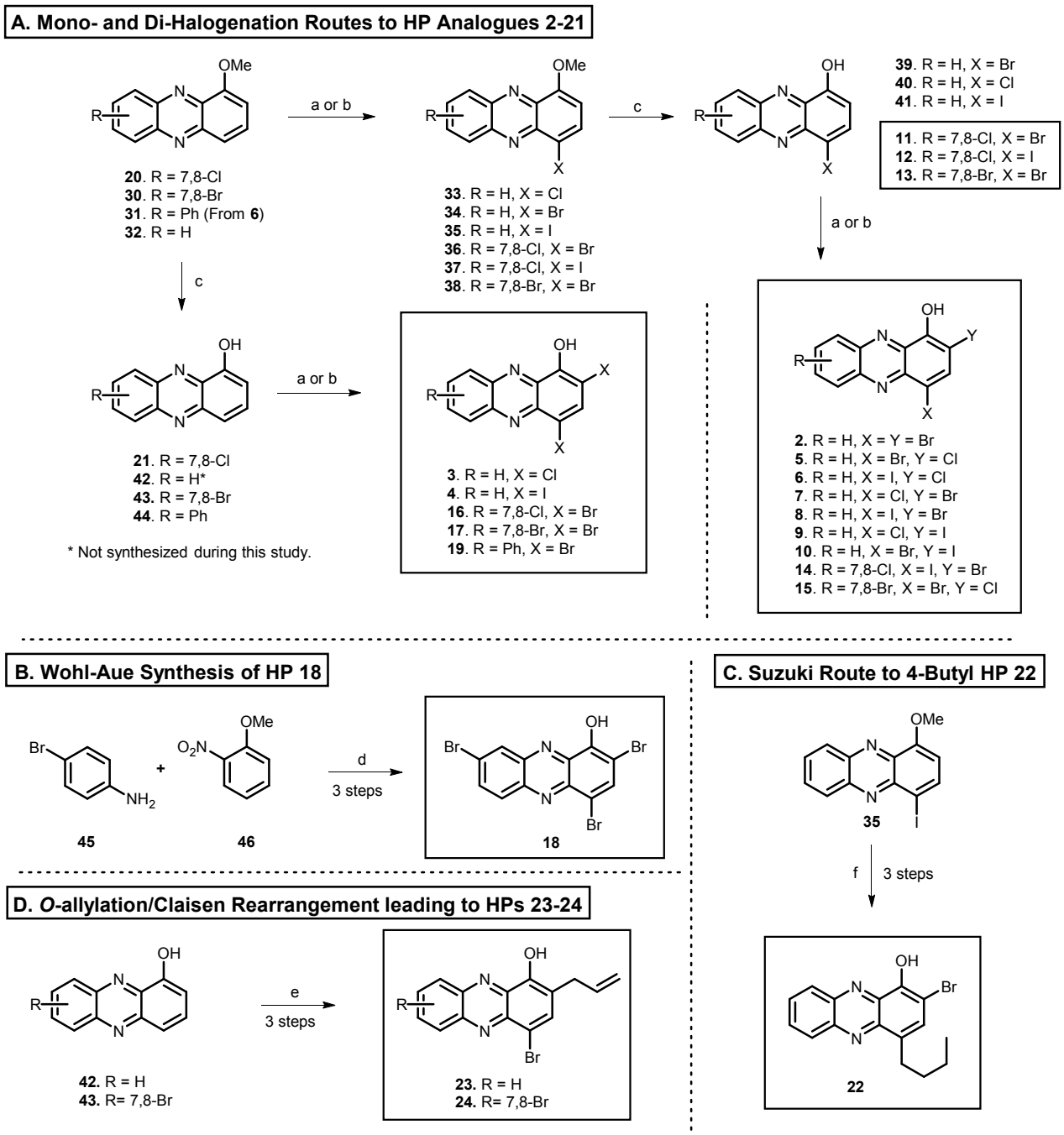

Scheme 1. Reagents and conditions: (a) NBS, NCS, or NIS, CH_2Cl_2, 19-96%; (b) KI, $NaIO_4$, NaCl, AcOH:H_2O (9:1), 86%; (c) BBr_3, CH_2Cl_2, -78 °C to r.t., 65-99%; (d) (i) KOH, PhMe, reflux, 2%; (ii) BBr_3, CH_2Cl_2, -78 °C to r.t., 99%; (iii) NBS, CH_2Cl_2, 46%; (e) (i) allyl bromide, K_2CO_3, acetone, reflux, 85-88%; (ii) microwave irradiation, EtOH, 99%; (iii) NBS, CH_2Cl_2, 39-99%; (f) (i) *n*-butylboronic acid pinacol ester, 20 mol% $Pd(PPh_3)_4$, NaOH, PhMe:H_2O (2:1), 36%; (ii) BBr_3, CH_2Cl_2, 90%; (iii) NBS, CH_2Cl_2, 53%.

Table 1. Summary of gram-positive antibacterial activities (MIC values reported) and HeLa cell cytotoxicity of HP analogues. All biological results in this table are reported in micromolar (μM) concentrations.

Compound	MRSA-2	MRSA BAA-1707	MRSA BAA-44	*S. epidermidis* 12228	MRSE 35984	VRE 700221	*M. tuberculosis* H37Ra	HeLa Cytotox. IC_{50} (μM)
2	1.56	1.17[a]	1.17[a]	1.17[a]	1.56	6.25	25	> 100
3	3.13	3.13	3.13	3.13	3.13	12.5	--	--
4	3.13	3.13	3.13	1.56	1.17[a]	6.25	--	> 100
5	2.35[a]	1.56	3.13	3.13	1.56	6.25	--	> 100
6	1.56	1.56	1.56	1.56	1.56	6.25	--	> 100
7	1.56	0.78	1.56	2.35[a]	1.56	6.25	--	> 100
8	0.78	1.17[a]	1.17[a]	0.78	1.56	6.25	--	> 100
9	25	3.13	12.5	25	25	6.25	--	--
10	2.35[a]	0.78	0.78	1.56	4.69[a]	6.25	--	--
11	0.78	0.30[a]	1.17[a]	3.13	1.56	6.25	3.13	> 100
12	0.39	0.15[a]	0.39	0.39	0.78	3.13	3.13	> 100
13	1.56	0.56[a]	1.56	2.35[a]	3.13	6.25	--	--
14	3.13	0.30[a]	3.13	0.10[b]	3.13	0.10[b]	12.5	> 50[c]
15	12.5	18.8[a]	25	0.08[a]	0.30[a]	0.39	--	> 100
16	4.69[a]	25	50	0.08[a]	0.30[a]	0.39	6.25	> 100
17	6.25	12.5	25	0.08[a]	2.35[a]	0.39	> 50	> 100
18	0.78	0.20	0.78	3.13	3.13	0.78	--	--
19	> 100	50	75[a]	12.5	18.8[a]	9.38[a]	--	--
20	> 100	--	--	> 100	> 100	> 100	--	--
21	> 100	--	--	> 100	> 100	> 100	--	--
22	3.13	1.56	2.35[a]	1.56	0.59[a]	0.78	--	--
23	> 100	--	--	> 100	--	> 100	--	--
24	> 100	--	--	> 100	--	> 100	--	--
25	25	6.25	12.5	18.8[a]	18.8[a]	100	--	>100
26	3.13	1.56	1.56	6.25	3.13	12.5	--	--
27	9.38[a]	4.69[a]	6.25	12.5	9.38[a]	25	--	--
28	1.56	0.78	1.56	2.35[a]	0.78	6.25	> 50	> 100
29	0.78	0.78	0.78	0.78	0.30[a]	2.35[a]	25	> 100
Vancomycin	0.59[a]	0.39	0.39	1.17[a]	0.78	> 100	--	--
Linezolid	3.13	12.5	1.56	1.56	3.13	3.13	--	--
Daptomycin	4.69[a]	3.13	18.8[a]	6.25	12.5	--	--	--
Rifampin	0.10[b]	--	--	0.10[b]	0.10[b]	--	--	--
Ciprofloxacin	> 100	--	--	0.78	0.20	--	--	> 100
Streptomycin	--	--	--	--	--	--	1.32	--

Notes: [a] Midpoint value (2-fold range in MIC). [b] Lowest concentration tested. [c] No HeLa cell death at 50 μM with ~70% cell death at 100 μM.; MIC values were obtained from 2-6 independent experiments.

Table 2. Summary of biofilm eradication studies against MRSA, MRSE and VRE biofilms. All biological results in this table are reported in micromolar (μM) concentrations.

Compound	MRSA-2 MBC / MBEC	MRSA BAA-1707 MBC / MBEC	MRSA BAA-44 MBC / MBEC	MRSE 35984 MBC / MBEC	VRE 700221 MBC / MBEC	% Hemolysis at 200 μM
2	15.6 / 93.8[a]	62.5 / 375[a]	62.5 / 188[a]	23.5[a] / 250[b]	23.5[a] / 9.38[a]	≤ 1
3	62.5 / > 1000	--	--	--	--	≤ 1
4	31.3 / 93.8[a]	--	--	31.3[b] / 23.5[a]	23.5[a] / 15.6	≤ 1
5	62.5 / > 1000	--	--	31.3 / 375[a]	11.7[a] / 11.7[a]	≤ 1
6	15.6 / 125	--	--	--	--	5.1
7	46.9[a] / 375	--	--	11.7[a] / 46.9[a]	7.8[b] / 3.9	≤ 1
8	31.3 / 62.5	23.5[a] / 93.8[a]	46.9[a] / 93.8[a]	11.7[a] / 188[a]	3.0[a] / 5.9[a]	2.9
9	93.8[a] / 250	--	--	125 / 250	--	≤ 1
10	46.9[a] / 250	--	--	--	--	1.3
11	37.5[a] / 37.5[a]	--	--	37.5[a] / 100	100[b] / 25	2.7
12	25 / 37.5	75[a] / > 200	75[a] / > 200	9.38[a] / 75[a]	3.13 / 1.56	1.4
13	> 200 / > 200	--	--	> 200 / > 200	> 200 / > 200	≤ 1
14	3.13 / 9.38[a]	4.69[a] / 6.25	12.5 / 9.38[a]	1.56 / 2.35[a]	0.20[c] / 0.20[c]	2.7
15	25[b] / 25	--	--	1.56 / 3.13	--	2.1
16	18.8[a] / 50	6.25 / 12.5	18.8[a] / 12.5	1.56 / 4.69[a]	0.39 / 0.39	≤ 1
17	37.5[a] / 50	6.25 / 50	50 / 37.5[a]	1.56 / 6.25	0.39 / 0.39	≤ 1
18	50 / 25	12.5 / 12.5	9.38[a] / 9.38[a]	37.5[a] / 25	1.56[b] / 0.59[a]	2.1
19	200 / > 200	--	--	--	--	≤ 1
22	46.9[a] / 188[a]	46.9[a] / 62.5	--	11.7[a] / 23.5[a]	2.0 / 2.0	11.5
25	1500[a] / > 2000	--	--	--	--	1.8
26	> 2000 / > 2000	--	--	750[a] / > 1000	--	≤ 1
27	125[b] / 1500	--	--	--	--	≤ 1
28	93.8[a] / 93.8[a]	--	--	23.5[a] / 125	--	1.2
29	23.5[a] / 188[a]	--	--	9.38[a] / 93.8[a]	2.0 / 1.5[a]	≤ 1
64 (QAC-10)	31.3[b] / 125	--	--	31.3 / 31.3	3.0[a] / 3.0[a]	> 99
CCCP	31.3 / 1000	--	--	31.3 / 93.8[a]	--	3.5
NAC	> 2000 / > 2000	--	--	> 2000 / > 2000	> 2000 / > 2000	--
Pyrazinamide	> 2000 / > 2000	--	--	--	--	--
Vancomycin	3.0[b] / > 2000	3.9 / > 2000	7.8 / > 2000	3.0[a] / > 2000	> 200 / 150	≤ 1
Daptomycin	62.5[b] / > 2000	125 / > 2000	--	--	--	1.7
Linezolid	15.6 / > 2000	31.3 / > 2000	--	--	4.69[b] / 1.56	≤ 1
Doxycycline	2.0 / 46.9[a]	--	--	--	--	--
Rifampin	2.0 / 46.9[a]	--	--	3.0[a] / 15.6[b]	--	--
EDTA	2000 / > 2000	--	--	1000 / > 2000	--	3.0

Notes: [a] midpoint value for independent experiments that gave a 2-fold range; [b] corresponds to a 4-fold range in independent experiments; [c] lowest concentration tested; MBC/MBEC values were obtained from 2-6 independent experiments.

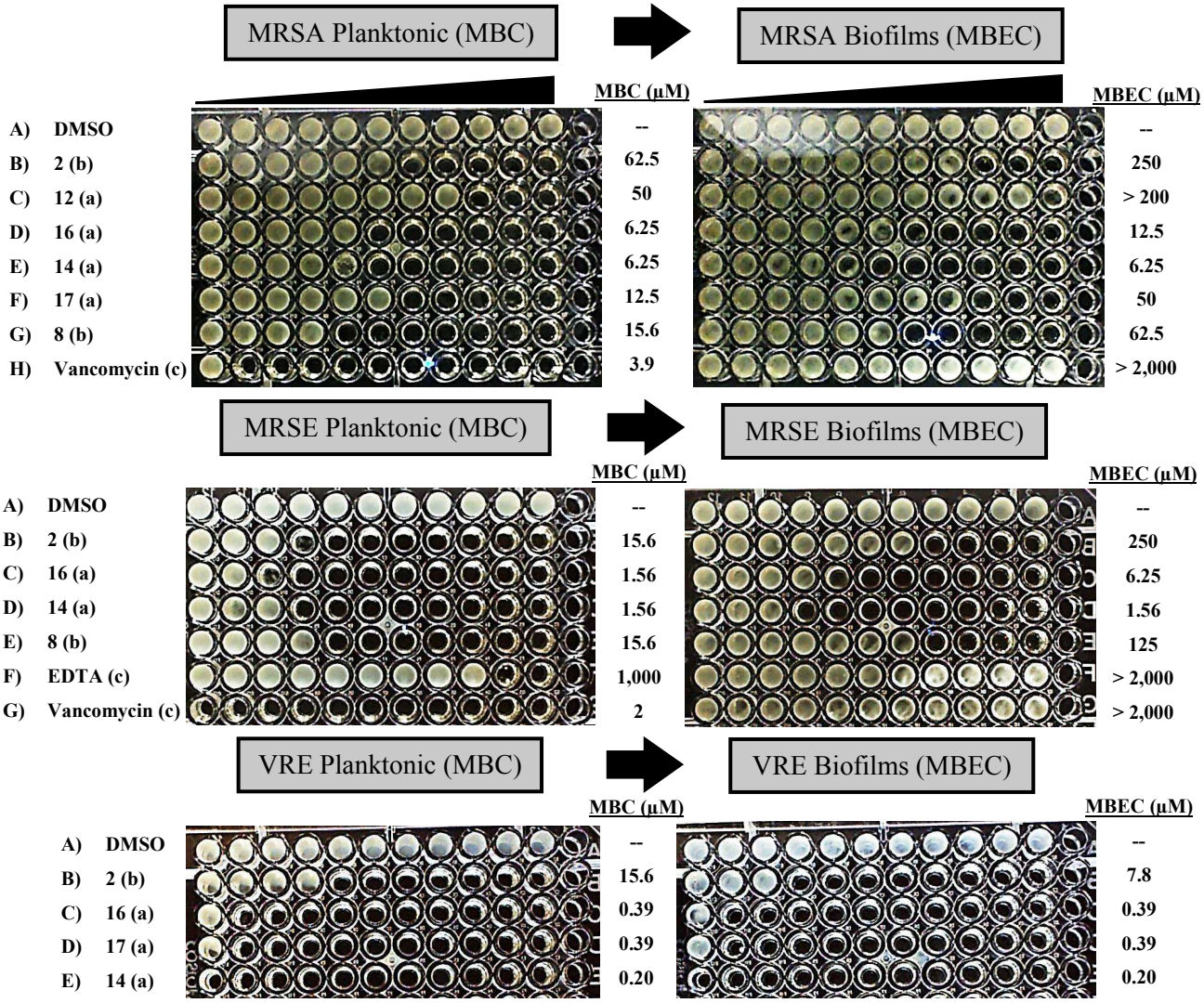

Figure 3. Calgary Biofilm Device assays to quantify planktonic (MBC) and biofilm (MBEC) killing efficiencies against MRSA-2, MRSE and VRE.

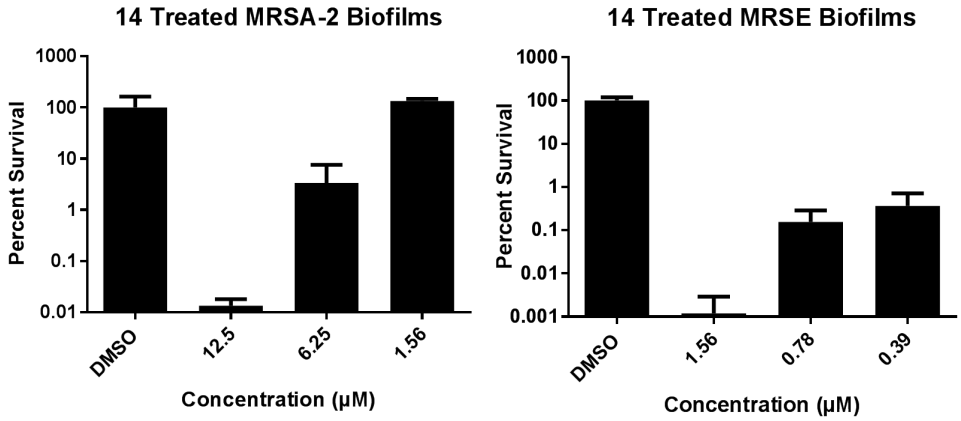

Figure 4. Biofilm cell killing (CFU/mL) for HP **14** obtained by colony counts from Calgary Biofilm Device pegs.

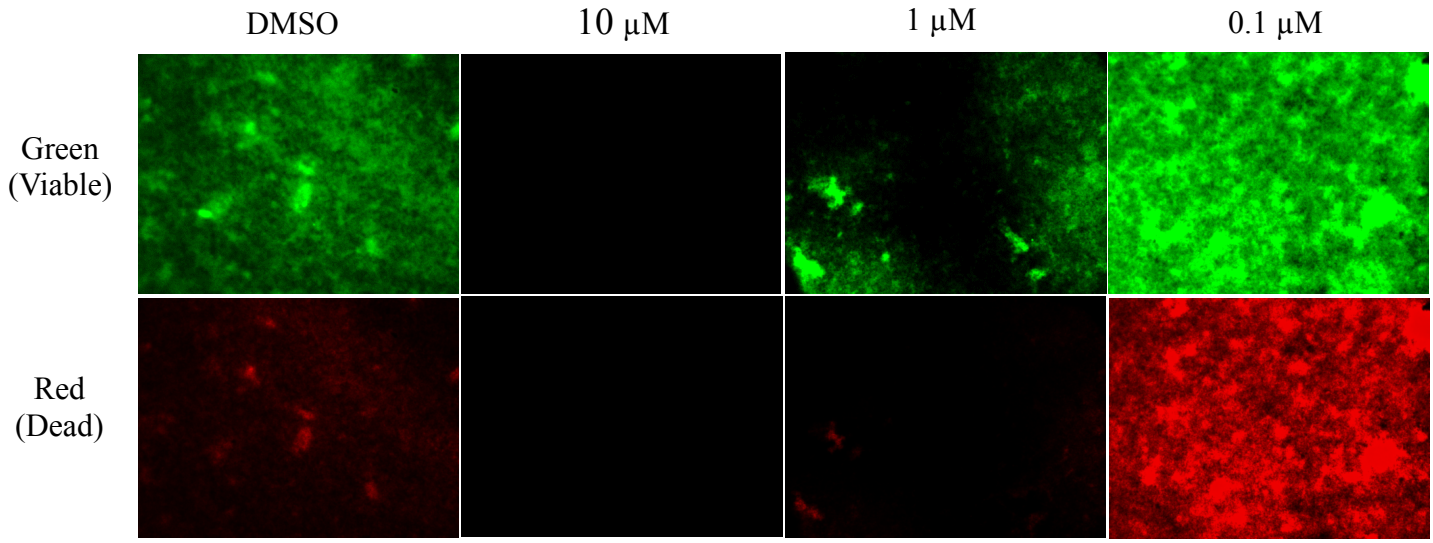

Figure 5. Live/dead staining of established MRSE 35984 biofilms treated with HP **14**.

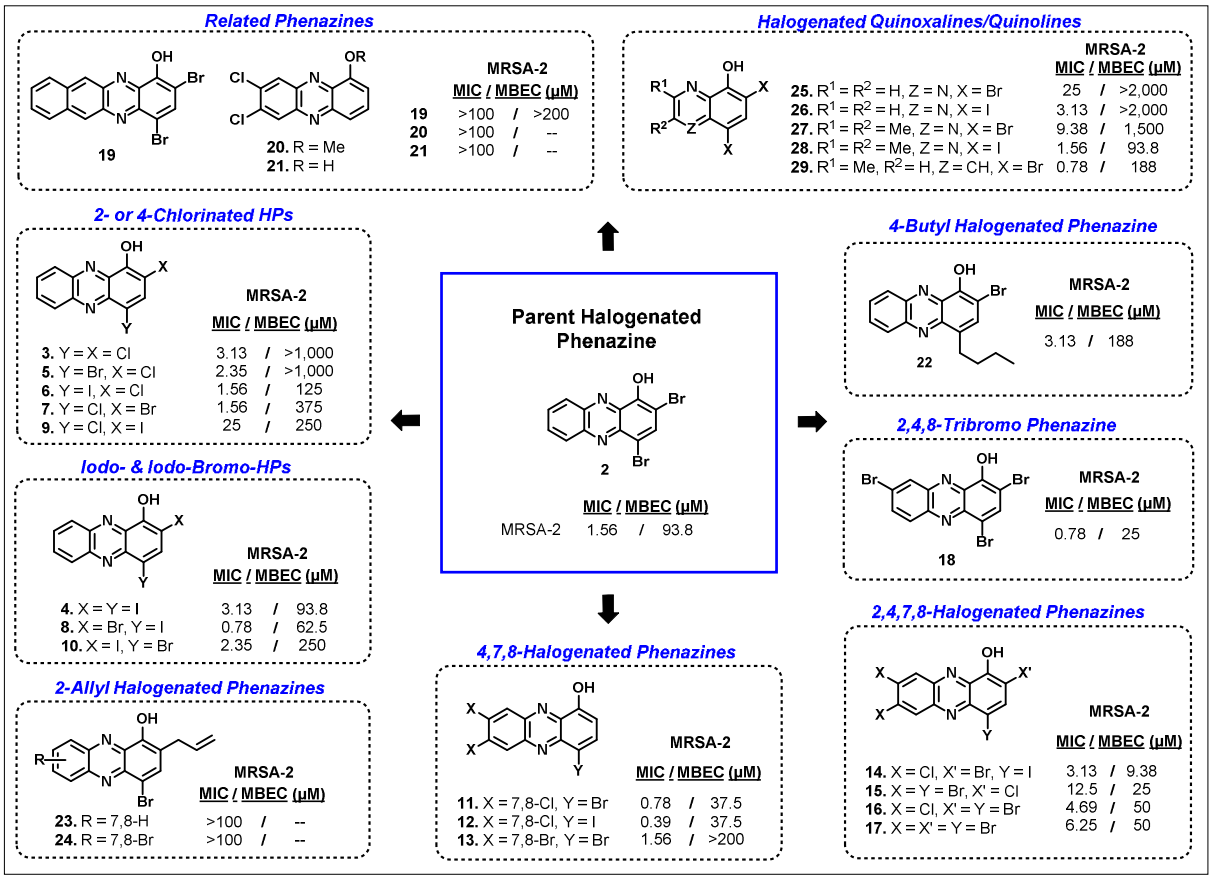

Figure 6. Diverse sub-classes of HP analogues with antibacterial and biofilm eradication activities against MRSA-2.

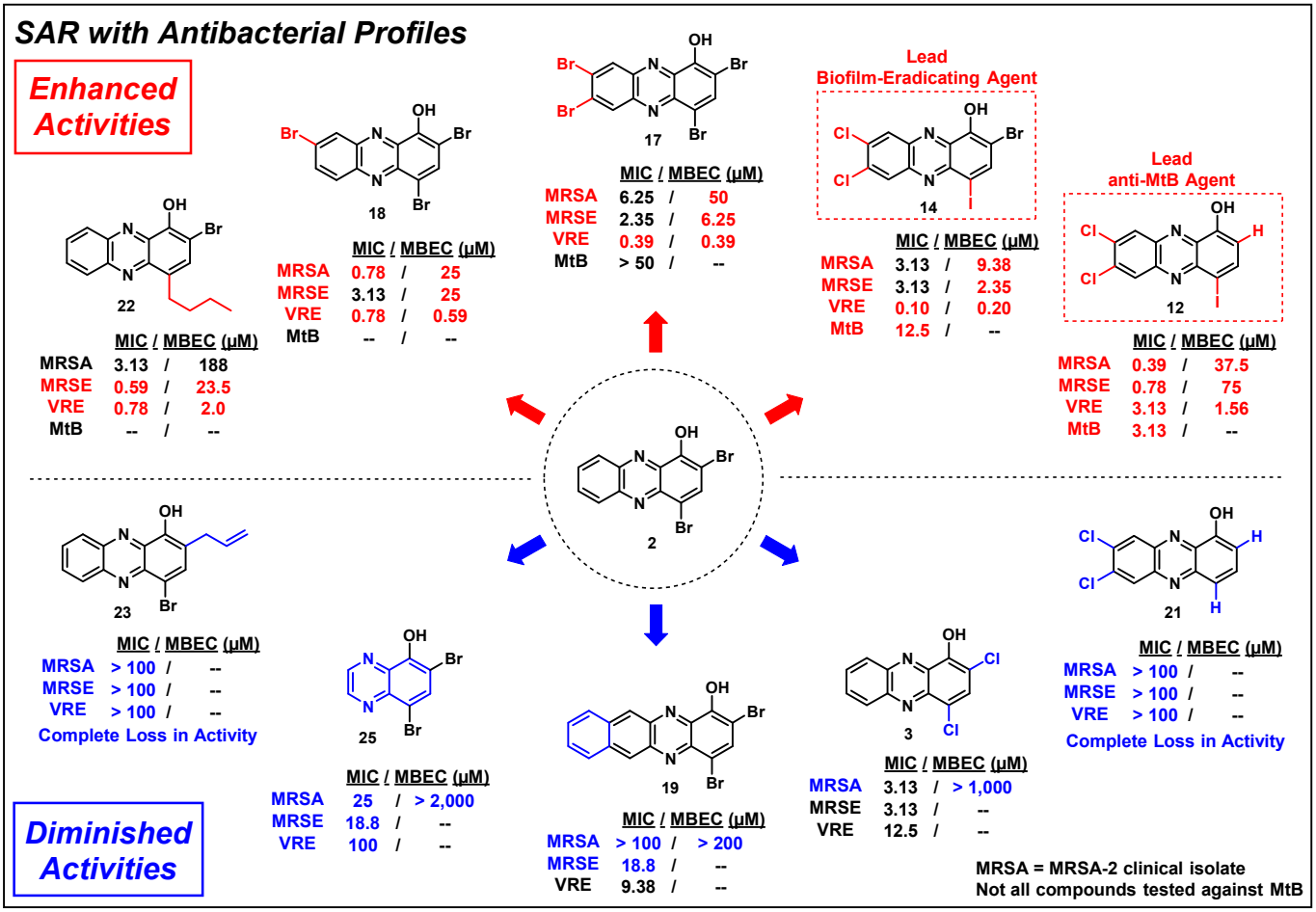

Figure 7. Detailed structure-activity relationships and antibacterial profiles of select halogenated phenazine analogues against MRSA, MRSE, VRE and MtB.

Table 3. Preliminary mechanistic studies, determination of solubility and pKa for select HP analogues.

	MRSA-2 (concentrations in μM)								
Compound	MIC	MIC w/ Tiron	Fold Δ	MIC w/ Cu^{2+}	Fold Δ	MIC w/ Fe^{2+}	Fold Δ	[aq. soluble][c]	pKa[d]
2	1.17[a]	1.17[a]	n.a.	75[a]	+ 48	3.13	+ 2	250 μM	6.74
8	1.17[a]	0.78	n.a.	50	+ 32	6.25	+ 5	--	--
11	0.78	--	--	--	--	--	--	200 μM[b]	8.42
12	0.59[a]	0.20	- 3	2.35[a]	+ 6	3.13	+ 5	200 μM[b]	7.70
13	12.5	0.10[b]	- 125	> 100	+ 8	25	+ 2	--	--
14	6.25	--	--	100	+ 16	18.8[a]	+ 3	200 μM[b]	6.95
15	3.13	0.20	- 16	> 100	+ 32	--	--	--	--
28	1.17[a]	0.78	n.a.	0.78	n.a.	4.69[a]	+ 4	--	--
8-HQ	6.25	>100	+ 16	3.13	n.a.	6.25	n.a.	--	--
Tetracyc.	1.17[a]	--	--	1.56	n.a.	18.8[a]	+ 16	--	--
Daptomy.	6.25	--	--	12.5	n.a.	6.25	n.a.	--	--
Linezolid	6.25	--	--	--	--	6.25	n.a.	--	--
4-nitrophenol	--	--	--	--	--	--	--	--	7.62

Note: "Fold Δ" denotes the change in antibacterial activity according to MIC values; (+) for increase in MIC value/loss of antibacterial activity; (-) for decrease in MIC value/increase of antibacterial activity; (n.a.) corresponds to insignificant changes in MIC values (< 2-fold changes); (--) not tested. 8-HQ is 8-hydroxyquinoline (positive control). [a] midpoint value for three independent experiments that gave a 2-fold range, [b] highest concentration tested, [c] determined under MIC assay conditions (16 hours, 37° C in media), [d] calculated pKa values, 4-nitrophenol was used for method validation.

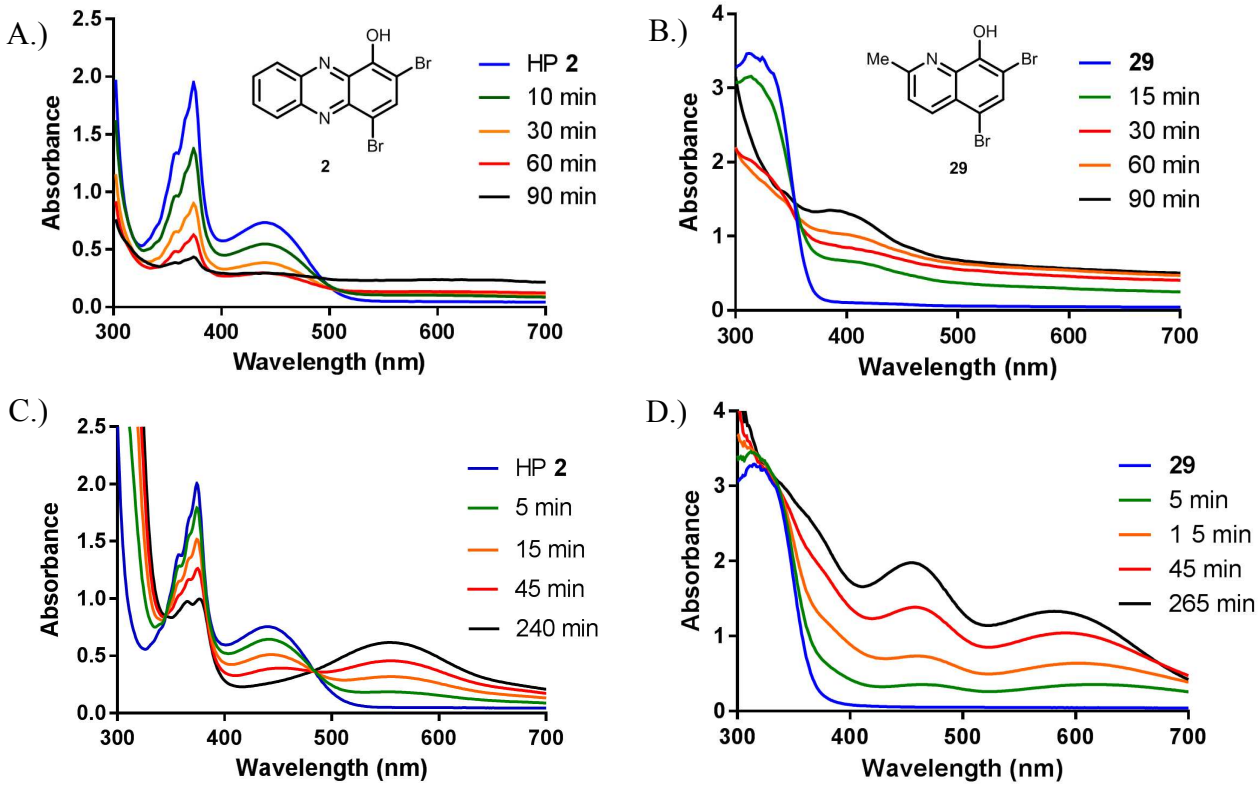

Figure 8. UV-Vis analysis of metal chelation with **2** and **29**. A.) HP **2** binding copper(II) resulting in a loss of absorbance due to complex precipitation (insoluble). B.) Halogenated quinoline **29** binding copper(II) results in a shift in absorbance, which remains soluble. C.) HP **2** binds iron(II) resulting in a shift in absorbance corresponding to a soluble HP-iron(II) complex (λ_{max} = 550 nm). D.) **29** binding iron(II) resulting in a shift in absorbance.

Structure-Activity Relationships of a Diverse Class of Halogenated Phenazines that Targets Persistent, Antibiotic-Tolerant Bacterial Biofilms and *Mycobacterium tuberculosis*

Corresponding author: Robert W. Huigens III